

Supporting Information

Metal Organic Framework Catalyzed Selective Oxidation of Alcohols and Oxidative Cross-Coupling for the C-C and C-N Bond Forming Reactions

Sheik Allavudeen Abdul Rahman,^a Chandrima N. Patra,^a Goutam Kumar Kole,^b Silda Peters,^b Tumpa Sadhukhan,^b Baburaj Baskar^{*a}

^aLaboratory of Sustainable Chemistry, Department of Chemistry, College of Engineering and Technology, SRM Institute of Science and Technology, Kattankulathur – 603203, Tamilnadu, India. Ph. No: +91 -9444741149; e-mail: baskarb@srmist.edu.in

^bDepartment of Chemistry, College of Engineering and Technology, SRM Institute of Science and Technology, Kattankulathur – 603203, Tamilnadu, India.

Table of Contents

1. Crystallographic information of 3a	S2-S5
2. Computational details of 3a	S6-S9
3. Experimental investigation of 3a	S10-S11
4. ¹ H and ¹³ C NMR spectra of 2a-2m & 6a-6o	S12-S39
5. References	S40

1. Crystallographic data

Table SI-1: Crystallographic parameters for Co(btc)(bpy) catalyst (MOF-3a)

Compound	Co(btc)(bpy)
CCDC No.	2320389
Formula	C ₆₀ H ₆₂ Co ₃ N ₁₀ O ₂₂
Formula weight (g.mol ⁻¹)	1451.99
Temperature (K)	100(2)
Radiation, λ (Å)	Mo K α ($\lambda = 0.71073$)
Crystal Colour, habit	Violet, Block
Crystal size (mm ³)	0.435 × 0.110 × 0.085
Crystal system	Triclinic
Space Group	P $\bar{1}$
Unit cell dimensions	
<i>a</i> (Å)	14.2087(11)
<i>b</i> (Å)	15.1919(12)
<i>c</i> (Å)	16.8364(12)
α (°)	79.338(3)
β (°)	72.665(3)
γ (°)	69.525(3)
Volume (Å ³)	3236.7(4)
<i>Z</i>	2
Calculated density (Mg.m ⁻³)	1.490
μ (mm ⁻¹)	0.845
θ range (°)	2.545 to 25.760
Reflections collected	117105
Independent reflections	12357
Parameters/ restraints	1034 / 273
GooF on F ²	1.135
R ₁ [$I > 2\sigma(I)$] ^a	0.0578
wR ₂ (all data) ^b	0.1593

Table SI-2 Selected bond distance and bond angles for Co(btc)(bpy) catalyst (MOF-3a)

Atoms	Bond distance (Å)	Atoms	Bond angle (°)	Atoms	Bond angle (°)
Co1–O1_1	1.998(10)	O1_1–Co1–O1_6	91.5(4)	O6_4–Co2–N1_3	141.3(4)
Co1–O1_6	2.076(8)	O1_1–Co1–N1_5	95.0(5)	O5_1–Co2–N2_3	171.5(4)
Co1–N1_5	2.104(12)	O1_6–Co1–N1_5	111.3(4)	O1_4–Co2–N2_3	84.5(4)
Co1–N2_5	2.131(11)	O1_1–Co1–N2_5	170.2(4)	O6_4–Co2–N2_3	90.8(4)
Co1–O4_4	2.183(9)	O1_6–Co1–N2_5	89.6(4)	N1_3–Co2–N2_3	76.9(5)
Co1–O3_4	2.189(9)	N1_5–Co1–N2_5	75.6(5)	O5_1–Co2–O5_4	85.3(3)

Co1-C2_4	2.505(13)	O1_1-Co1-O4_4	94.0(4)	O1_4-Co2-O5_4	147.3(3)
Co2-O5_1	2.036(9)	O1_6-Co1-O4_4	149.9(4)	O6_4-Co2-O5_4	58.1(3)
Co2-O1_4	2.049(10)	N1_5-Co1-O4_4	97.8(4)	N1_3-Co2-O5_4	87.4(3)
Co2-O6_4	2.080(8)	N2_5-Co1-O4_4	89.9(4)	N2_3-Co2-O5_4	98.9(4)
Co2-N1_3	2.103(10)	O1_1-Co1-O3_4	92.3(4)	O6_1-Co3-O2_4	93.9(4)
Co2-N2_3	2.130(11)	O1_6-Co1-O3_4	91.1(3)	O6_1-Co3-O4_1	90.2(4)
Co2-O5_4	2.396(9)	N1_5-Co1-O3_4	156.3(4)	O2_4-Co3-O4_1	97.7(4)
Co3-O6_1	2.035(8)	N2_5-Co1-O3_4	97.4(4)	O6_1-Co3-N1_2	85.1(4)
Co3-O2_4	2.039(8)	O4_4-Co1-O3_4	59.1(3)	O2_4-Co3-N1_2	170.5(4)
Co3-O4_1	2.077(10)	O1_1-Co1-C2_4	91.2(4)	O4_1-Co3-N1_2	91.8(4)
Co3-N1_2	2.108(10)	O1_6-Co1-C2_4	120.2(4)	O6_1-Co3-N2_2	122.0(4)
Co3-N2_2	2.113(10)	N1_5-Co1-C2_4	128.0(4)	O2_4-Co3-N2_2	96.3(4)
Co3-O3_1	2.309(9)	N2_5-Co1-C2_4	96.6(4)	O4_1-Co3-N2_2	143.7(3)
		O4_4-Co1-C2_4	30.2(3)	N1_2-Co3-N2_2	76.4(4)
		O3_4-Co1-C2_4	29.1(3)	O6_1-Co3-O3_1	149.3(4)
		O5_1-Co2-O1_4	96.0(4)	O2_4-Co3-O3_1	90.1(3)
		O5_1-Co2-O6_4	97.7(4)	O4_1-Co3-O3_1	59.2(3)
		O1_4-Co2-O6_4	89.5(4)	N1_2-Co3-O3_1	95.6(4)
		O5_1-Co2-N1_3	95.9(4)	N2_2-Co3-O3_1	87.6(3)
		O1_4-Co2-N1_3	124.8(4)		

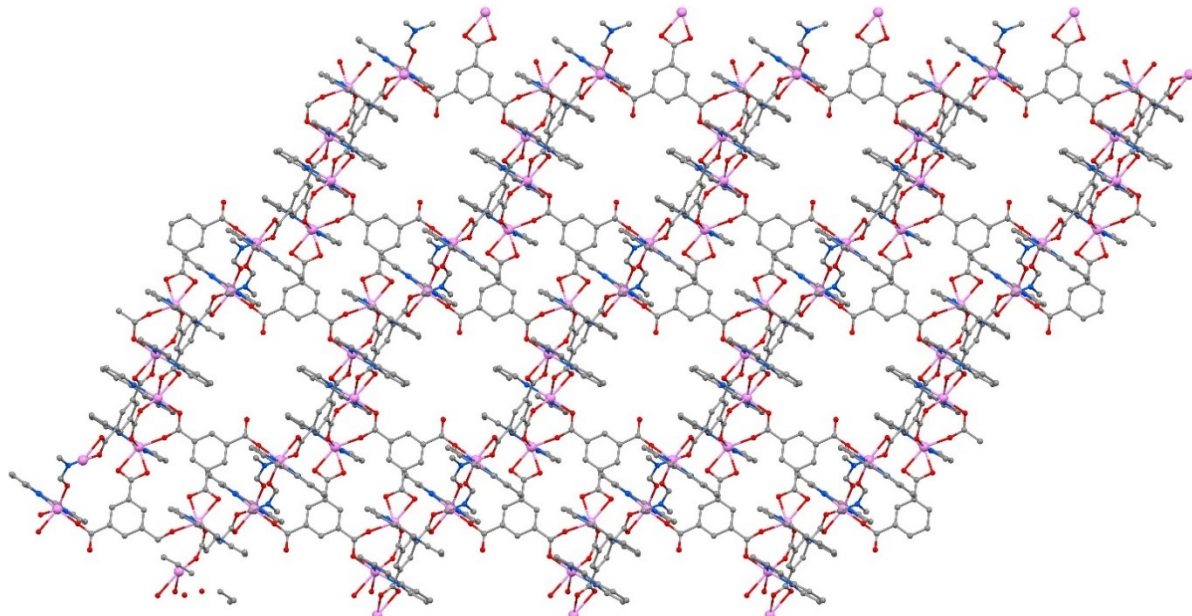


Figure SI-1: Two-dimensional coordination polymer structure of the catalyst, viewed approximately along ‘a’-axis. The solvent accessible void volume can be seen. Lattice solvents – DMF and water are not shown for clarity.

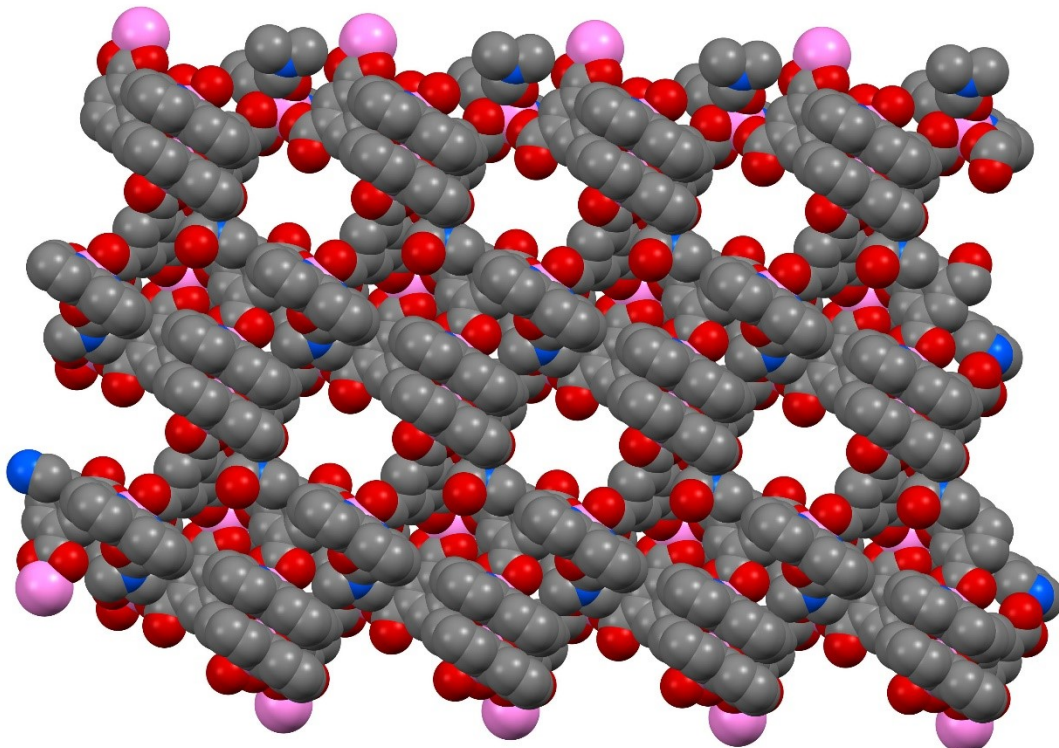


Figure SI-2: Two-dimensional coordination polymer structure of the catalyst. Solvent accessible void volume can be seen in the space filled model.

Analysis of PXRD

Crystals of coordination polymer **Co-MOF-3a** was ground into powder on a mortar and the obtained powder sample was analyzed for its powder x-ray diffraction patterns. The experimentally obtained patterns were plotted again the simulated patterns. The powdered sample showed moderate crystallinity and it matched quite well with the simulated patterns. For testing the crystallinity of the used catalyst, we have recorded the PXRD pattern of the catalyst used for five cycles. It showed significant crystallinity.

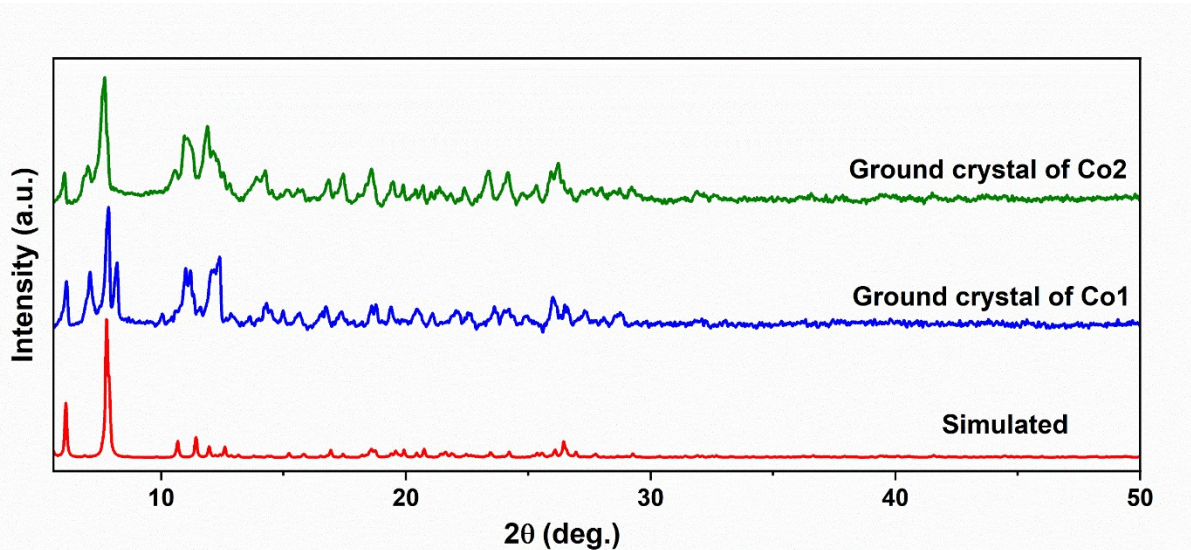
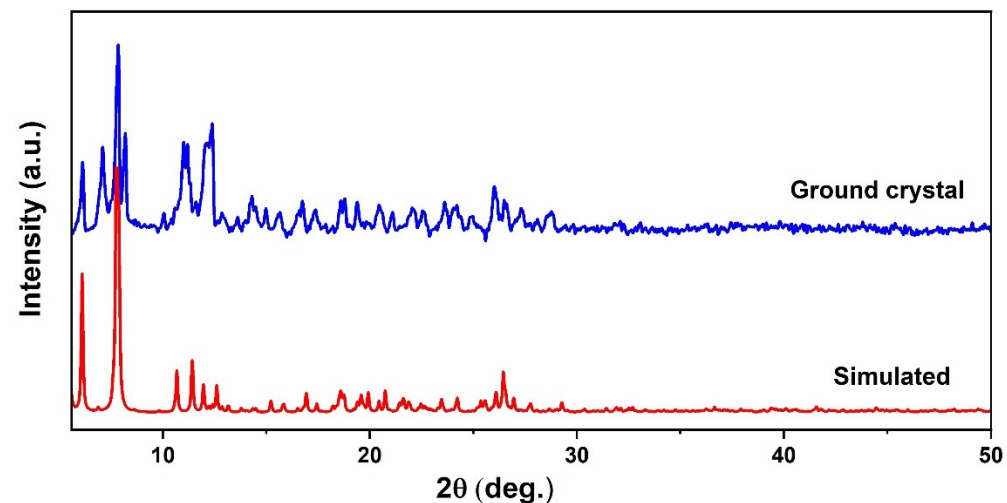


Figure SI-3: Simulated, experimentally observed PXRD patterns of **as synthesized Co-MOF-3a (Co-1)** and of the catalyst recovered after five cycles (**Co-2**) are shown..

Computational Details:

The unit cell of the Co(btc)(bpy) MOF was used for our calculations. All computational calculations were performed utilizing the Vienna ab initio simulation package (VASP).¹ The calculations were rooted in spin-polarized density functional theory (DFT). They relied upon a plane-wave basis set augmented by the projector-augmented wave (PAW)² technique to describe electron-ion interactions accurately. Geometry optimization of the MOF structure employed the generalized gradient approximation (GGA)³ functional, specifically the Perdew, Burke, and Ernzerhof (PBE)⁴ exchange-correlation functional. Grimme's DFT D3BJ correction⁵ was incorporated to account for dispersion forces, enhancing the accuracy of the results. The optimized geometry, illustrating the most stable arrangement of atoms, is represented in **Figure SI-4**. The energy and force convergence standards were established at 1×10^{-6} eV per unit cell and 1×10^{-2} eV per Å. The energy cutoff for plane-wave expansion was set at 520 eV, ensuring a comprehensive treatment of the electronic structure. The Brillouin zone was efficiently sampled using the Γ -centered k-grid scheme with a $4 \times 4 \times 4$ k-mesh, providing a suitable level of accuracy in reciprocal space. After optimization, the cell parameters and structural characteristics of the MOF were documented in **Tables SI(i) to SI(iii)**, along with atom type labels corresponding to **Figure SI5**. These tables provide comprehensive details of the final configuration of the MOF.

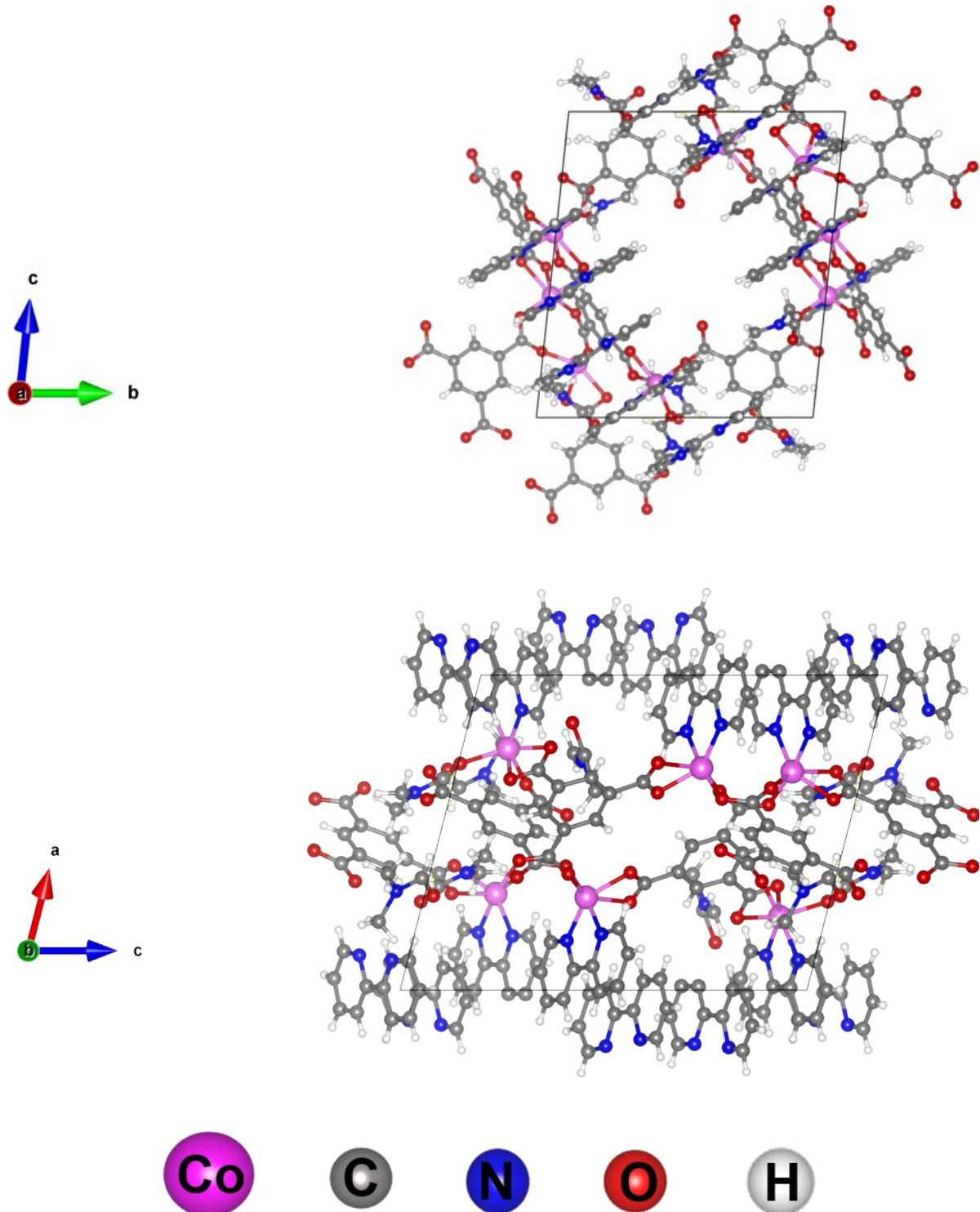


Figure SI-4. Optimized structure of MOF.

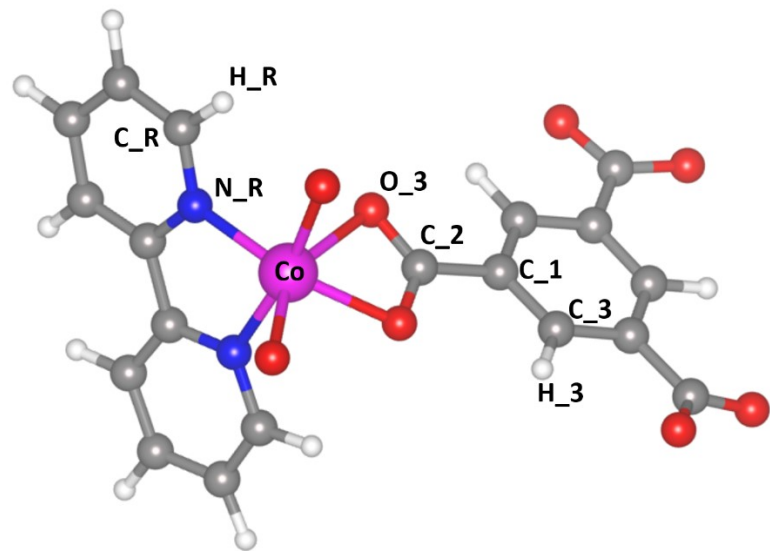


Figure SI-5. Atom-labelled unit of the MOF framework.

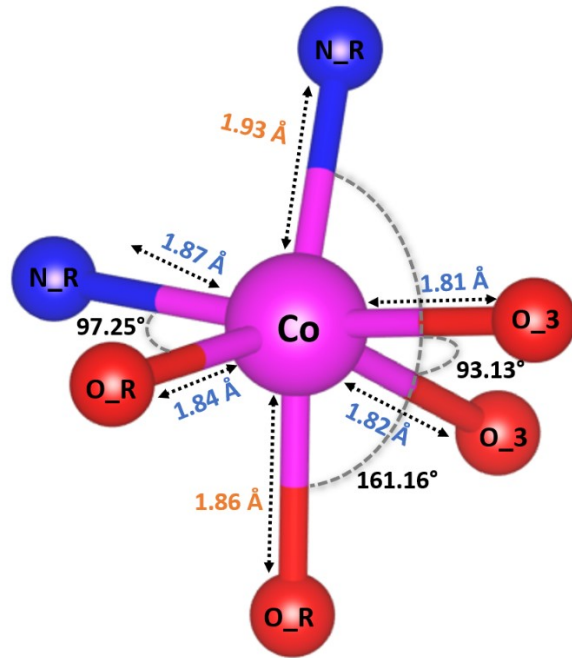


Figure SI-6: Coordination Alignment of metal Center (Co) with its bonded Atoms.

Table SI(i). MOF cell parameters taken from DFT optimization.

MOF	Lattice Size (Å)			Angle (°)			Cell Volume (Å ³)
	a	b	c	α	β	γ	
	14.20	15.59	16.95	78.36	72.54	68.94	3324.63

Table SI(ii). Average Bonding Parameters of the MOF.**Bonds**

a1	a2	Bond Length (Å)
Co	O_R	1.85
Co	O_3	1.82
Co	N_R	1.90
C_R	C_R	1.46
C_R	H_R	1.08
C_R	N_R	1.34
C_2	O_3	1.36
C_3	H_3	1.10
C_1	C_2	1.51
C_1	C_3	1.40

Table SI(iii). Average Bending Parameters for MOF.**Angles**

a1	a2	a3	Angle (°)
Co	O_R	O_R	145.9
Co	O_3	O_R	148.4
Co	N_R	O_R	154.5
C_R	C_R	C_R	111.3
C_R	C_R	H_R	107.2
C_R	N_R	C_R	120.0
C_R	C_R	N_R	153.7
C_2	O_3	Co	88.80
O_3	C_2	C_1	129.9
C_1	C_3	H_3	119.8
C_3	C_1	C_2	120.1
C_3	C_1	C_3	120.0

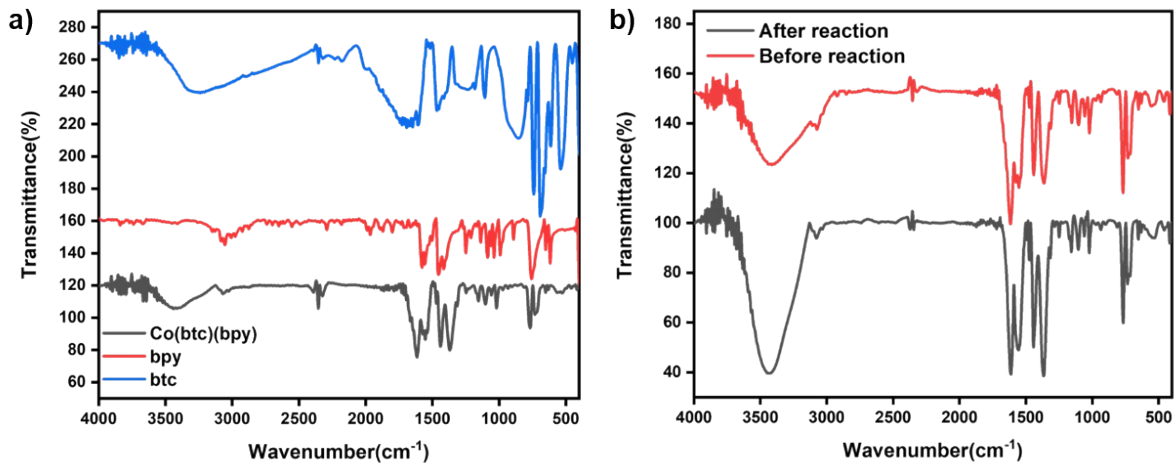


Fig SI-7. FTIR spectra of **a)** Co(btc)(bpy), btc and 2,2'-bpy **b)** reused catalyst after 5 cycles

Fig 7a shows the stacked FTIR spectra of btc, bpy and MOF-3a, a broad peak in 3400-3500 cm⁻¹ shows the stretching vibration of hydroxyl groups.⁶ The peak at 3100 shows the stretching frequency of sp² hybridized C-H while the stretching and bending vibrations of C=C in benzene tricarboxylic acid and 2,2'-bipyridine appear at 1450-1600 cm⁻¹ and 650-900 cm⁻¹, respectively. The stretching frequency of C=O has shifted to 1620 cm⁻¹ due to the coordination of oxygen to cobalt, which lowers the frequency as the strength of C=O bond in the carbonyl decreases.⁷ Fig 7b shows the IR spectra of reused catalyst after 5 cycles and it is observed that there is no change in FTIR absorption pattern

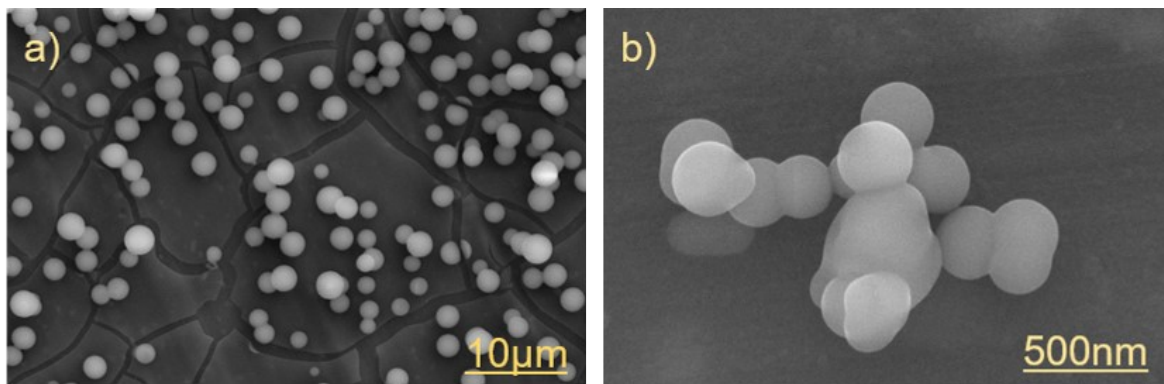


Fig SI-8. SEM images **(a)** and **(b)** of reused Co(btc)(bpy) catalyst after 5 cycles

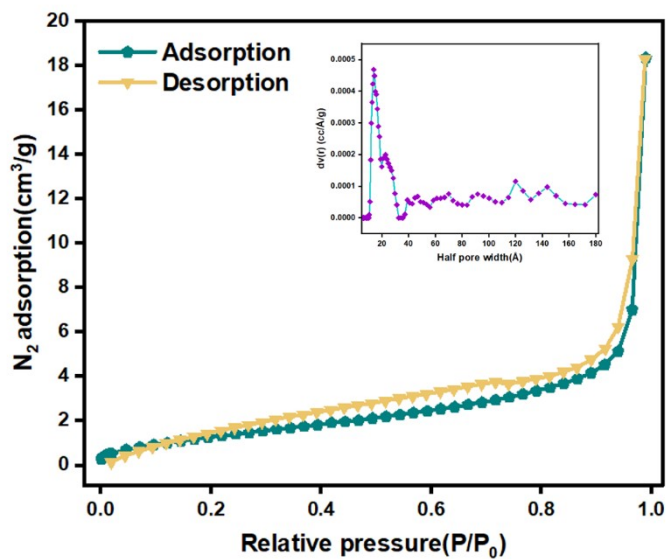
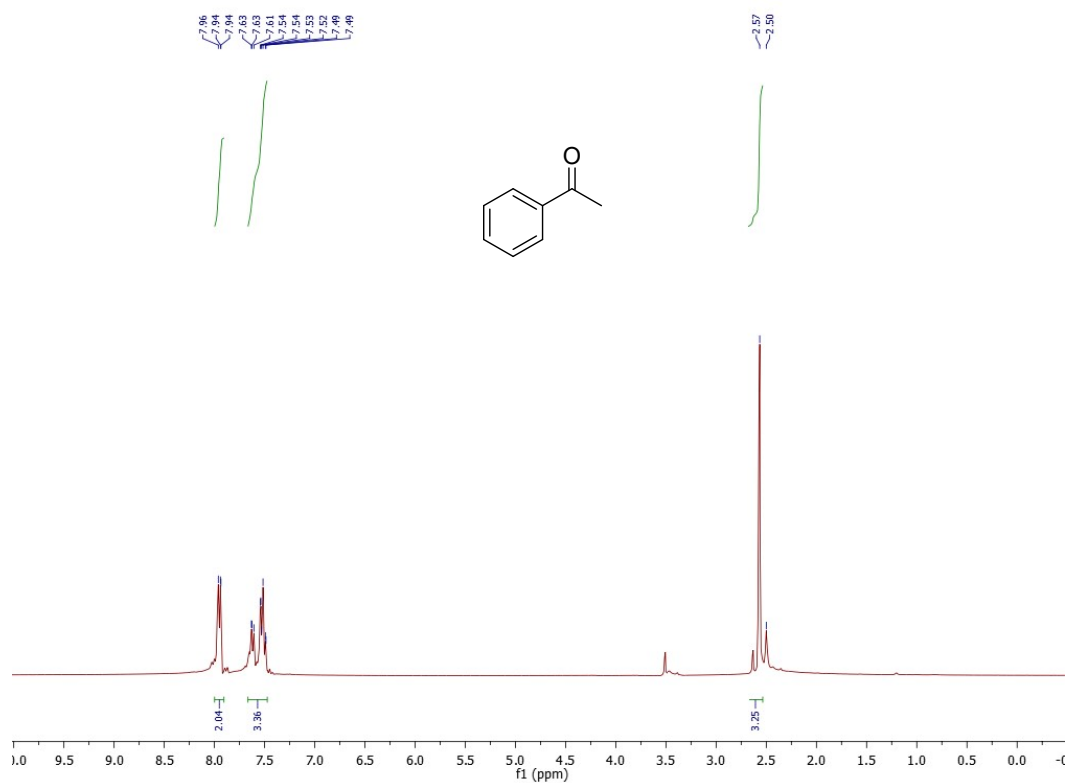
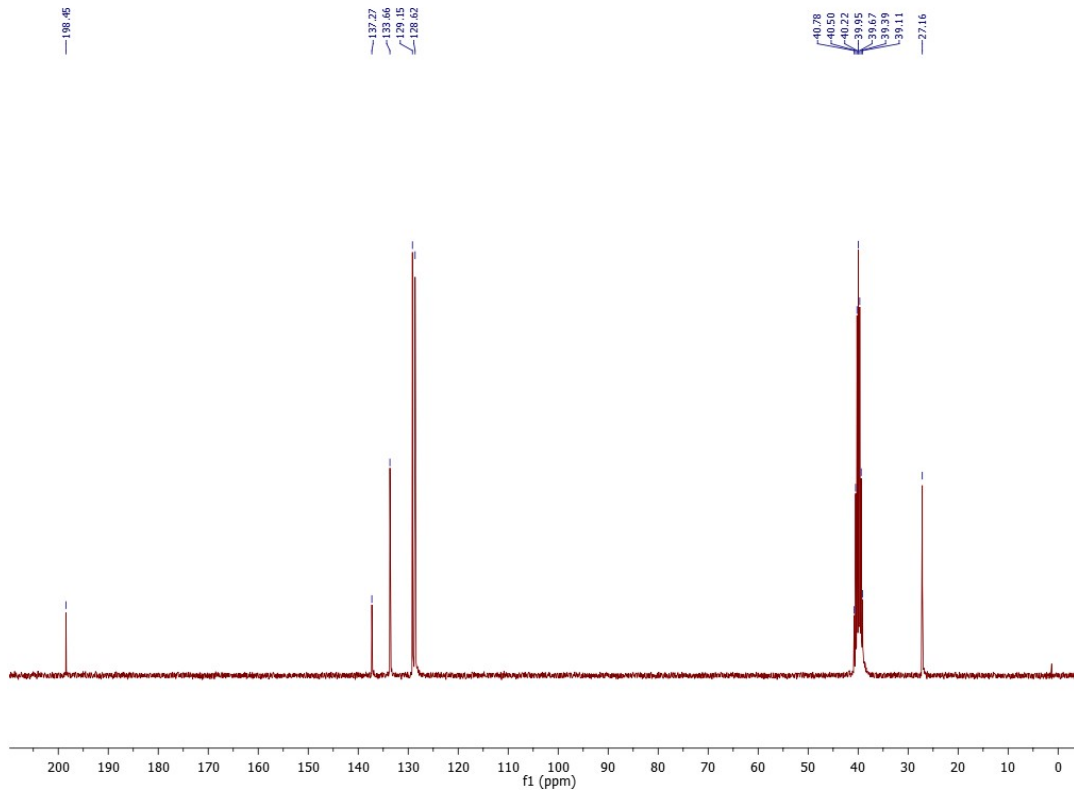


Fig SI-9: BET N_2 adsorption of Co-MOF-3a after 5 cycles

Acetophenone (2a)

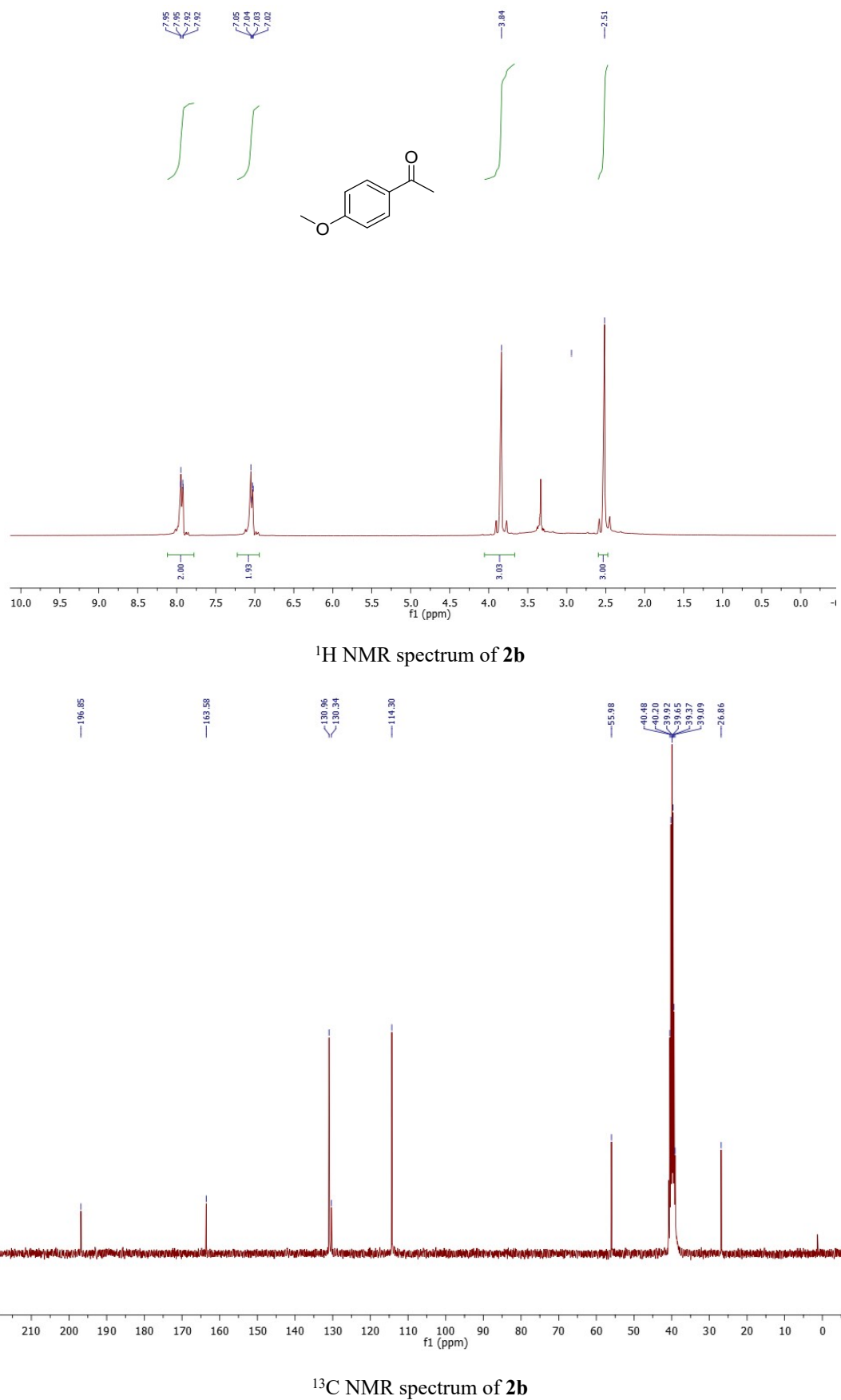


¹H NMR spectrum of 2a

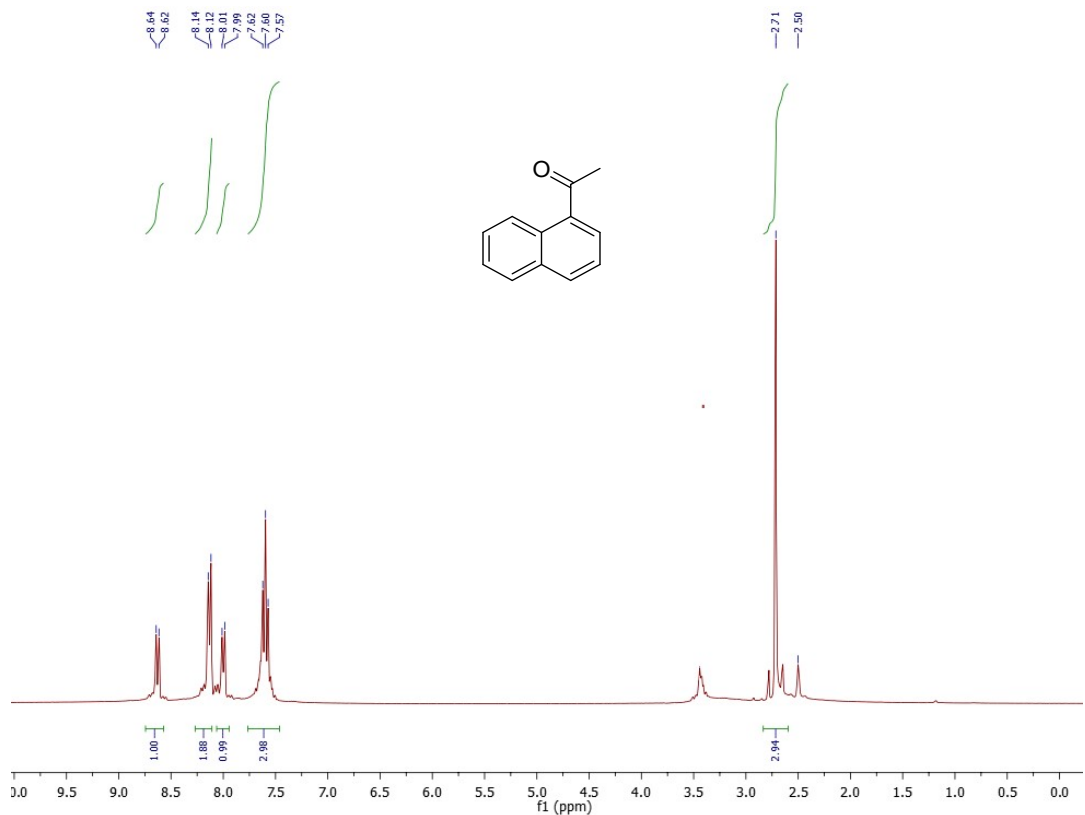


¹³C NMR spectrum of 2a

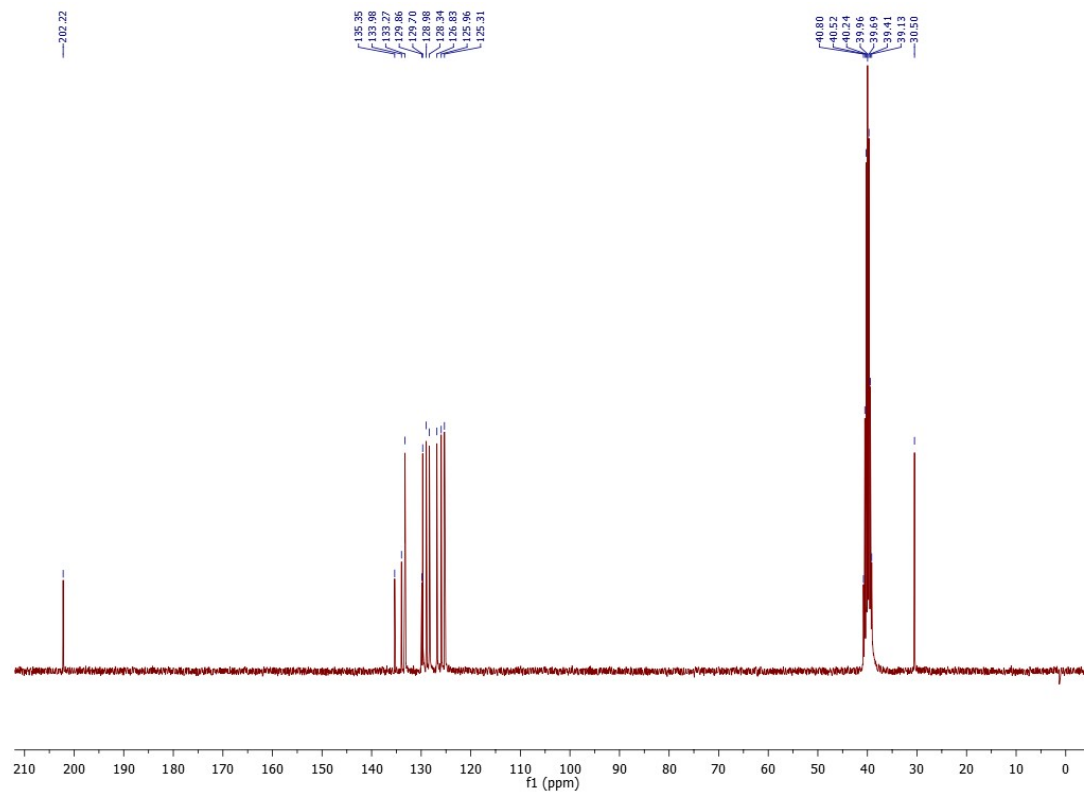
4-Methoxy acetophenone (2b)



1-Acetyl naphthalene(2c)

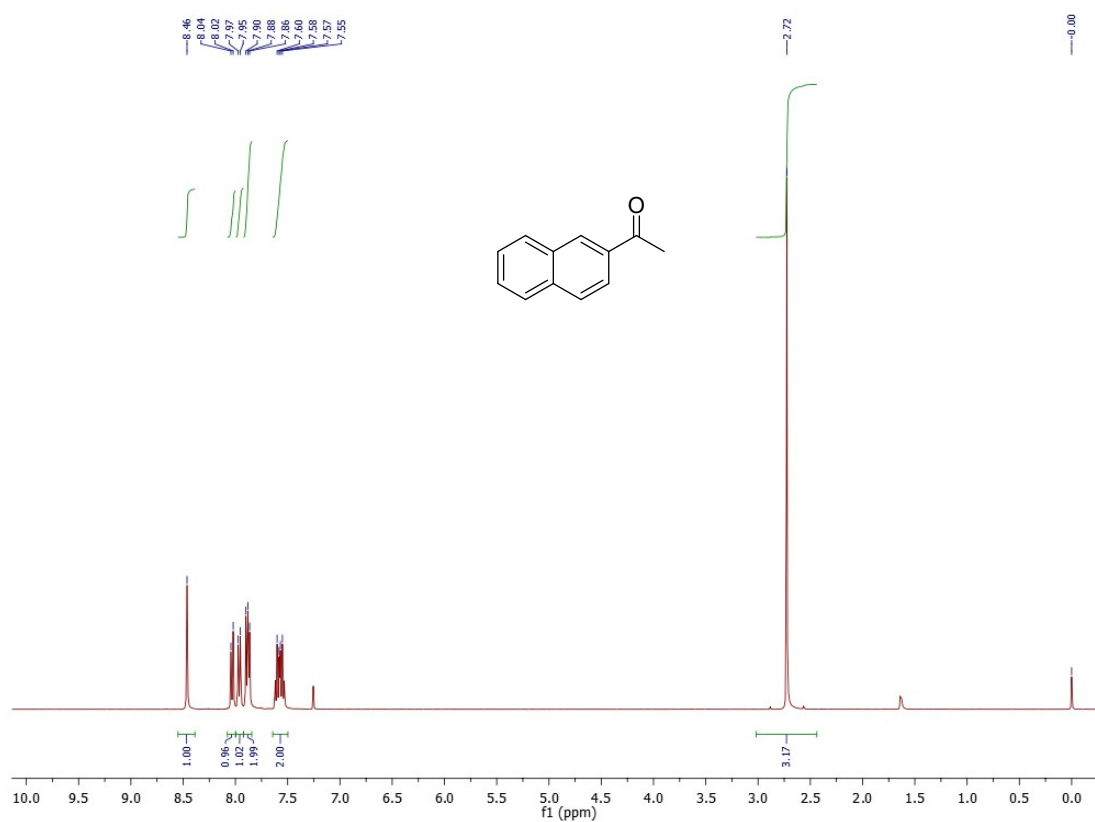


¹H NMR spectrum of **2c**

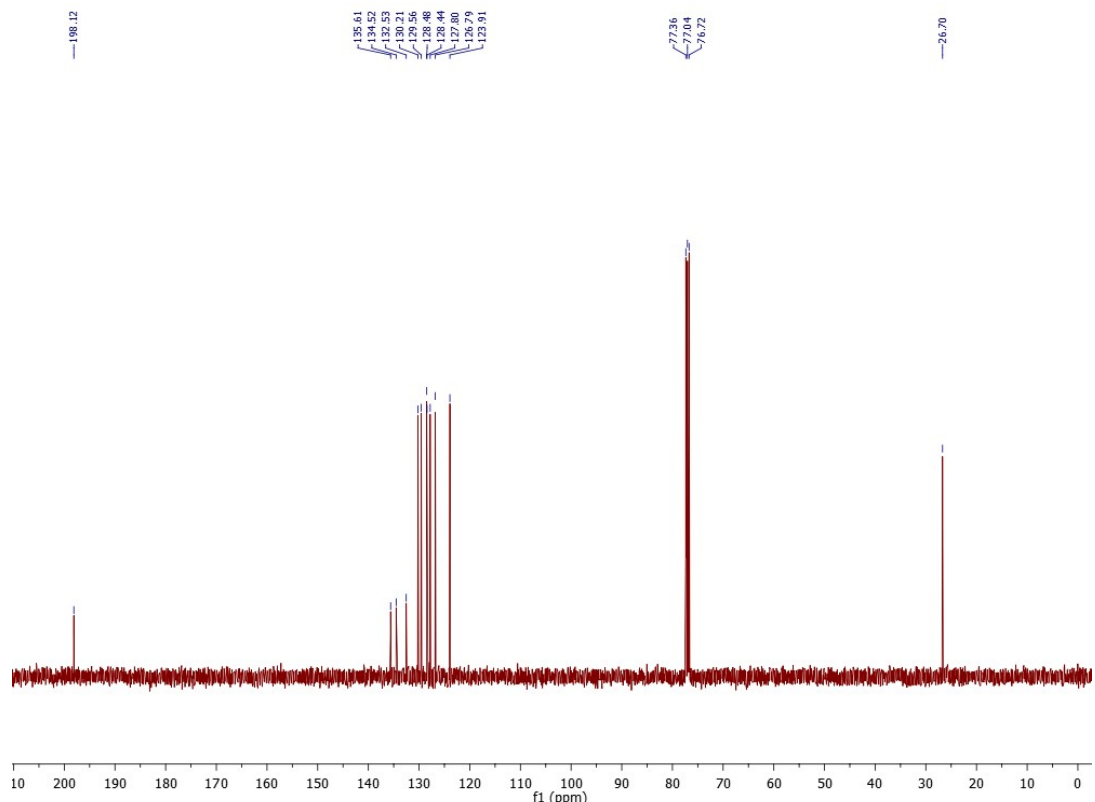


¹³C NMR spectrum of **2c**

2-Acetyl naphthalene(2d)

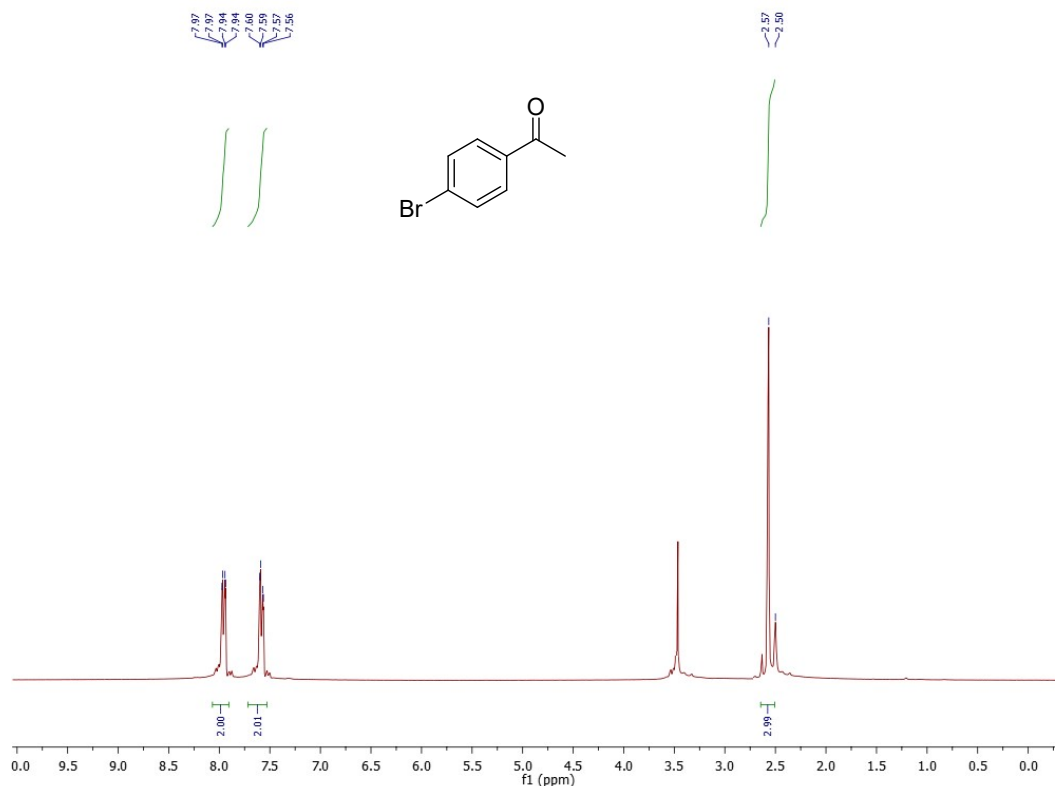


¹H NMR spectrum of 2d

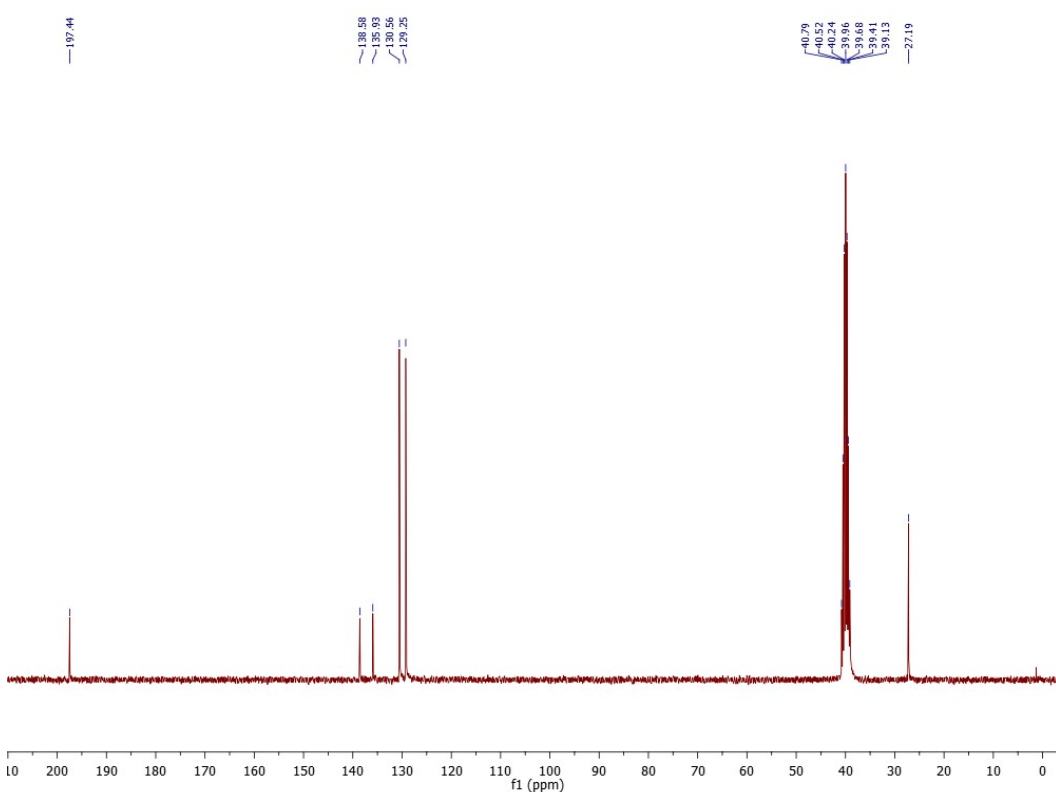


¹³C NMR spectrum of 2d

4-Bromo acetophenone (2e**)**

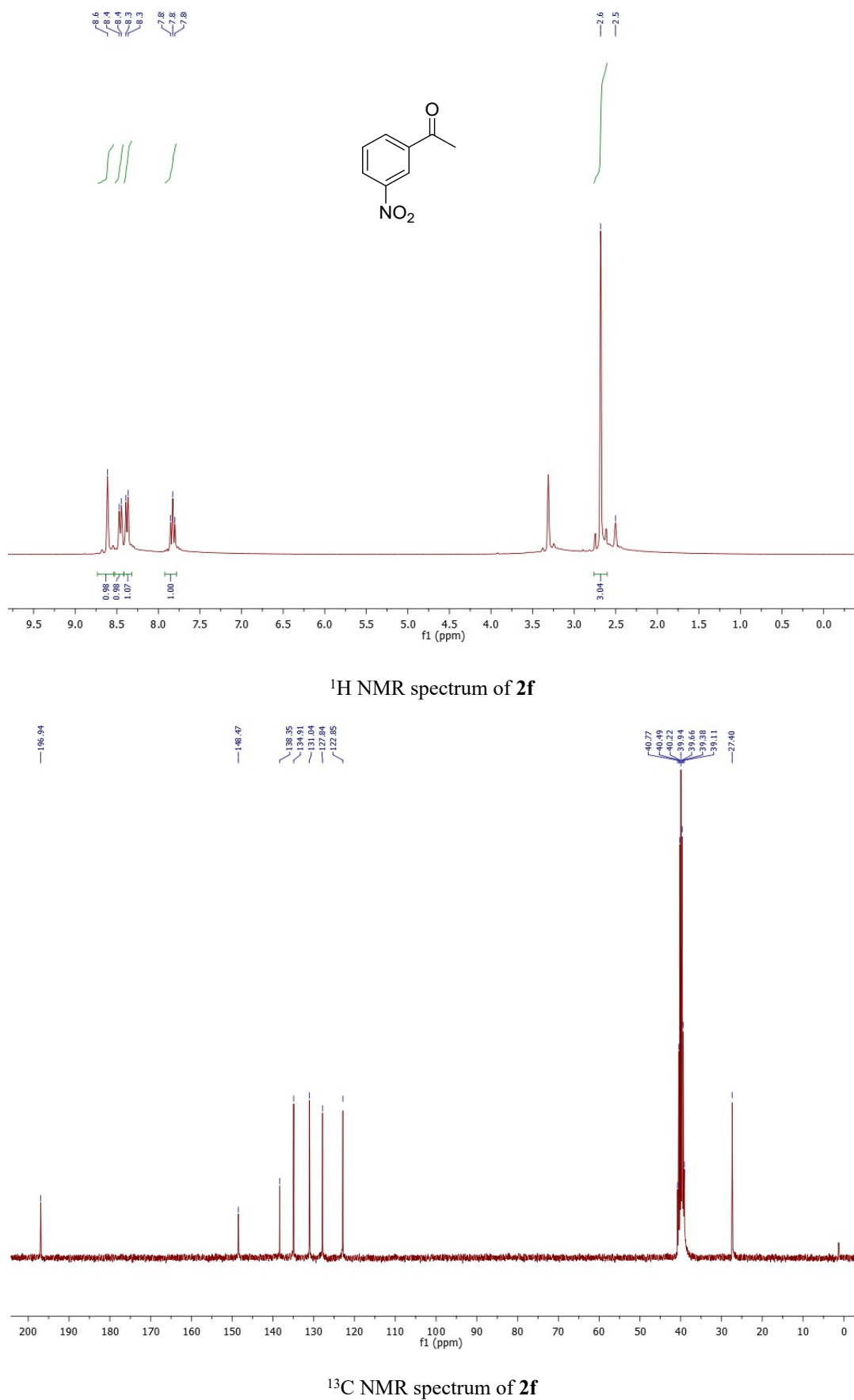


¹H NMR spectrum of **2e**



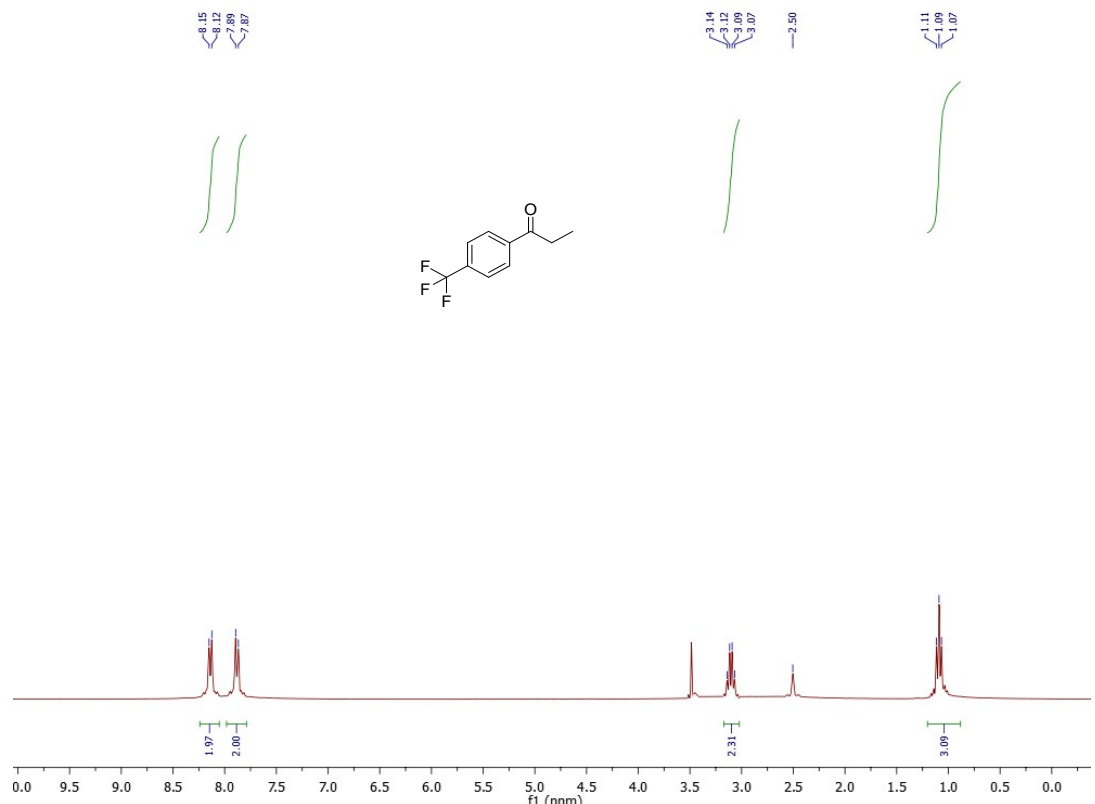
¹³C NMR spectrum of **2e**

3-Nitro acetophenone(2f)

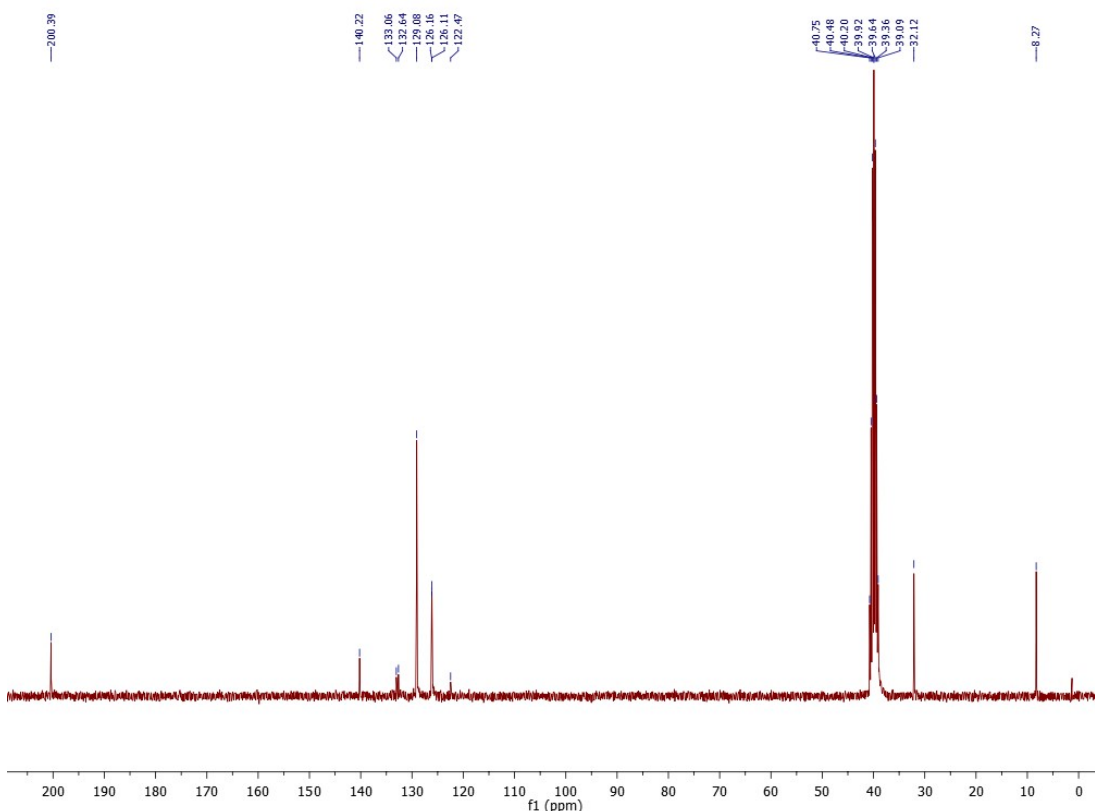


¹³C NMR spectrum of **2f**

4-Trifluoroethylphenone (2g)

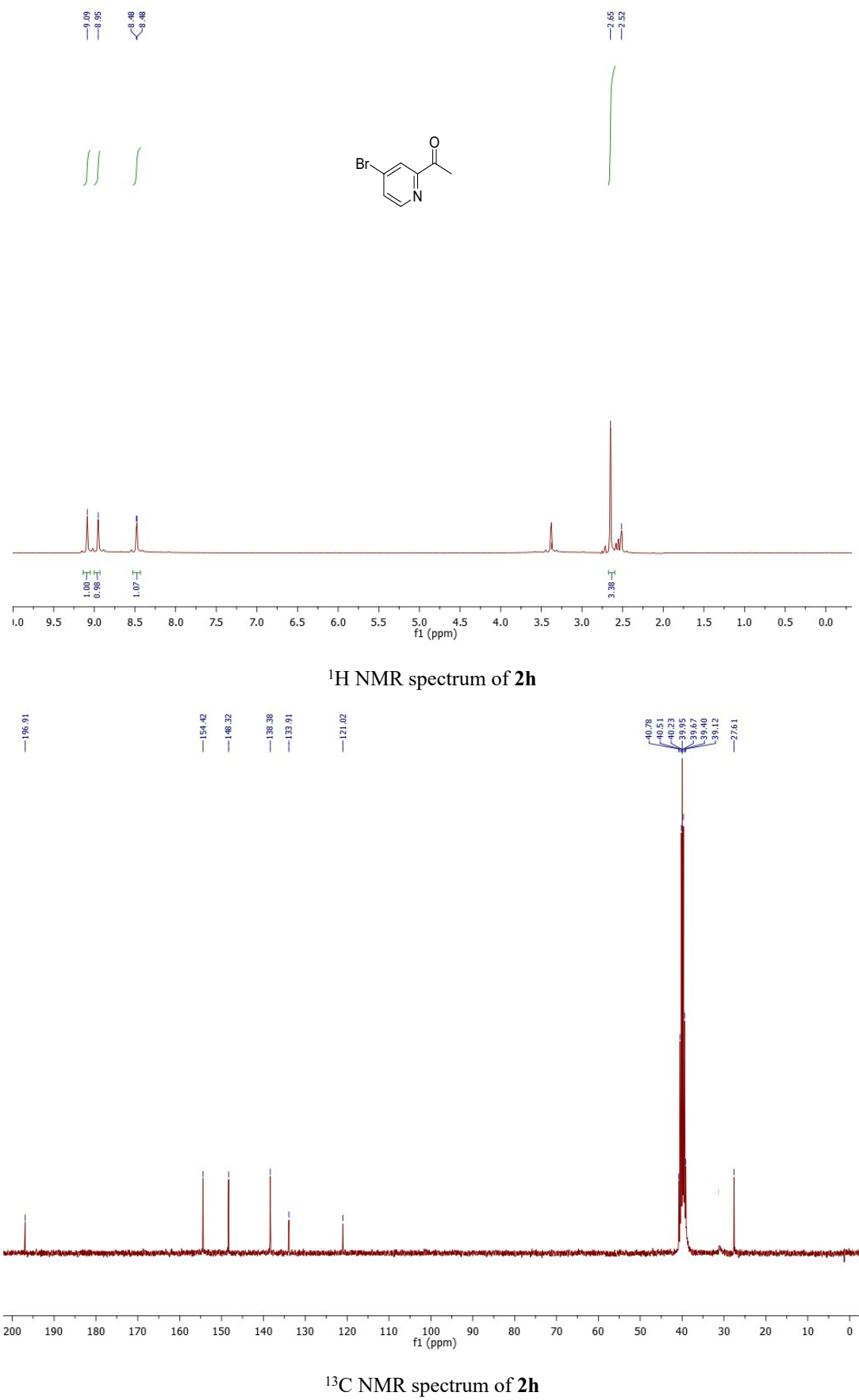


¹H NMR spectrum of 2g

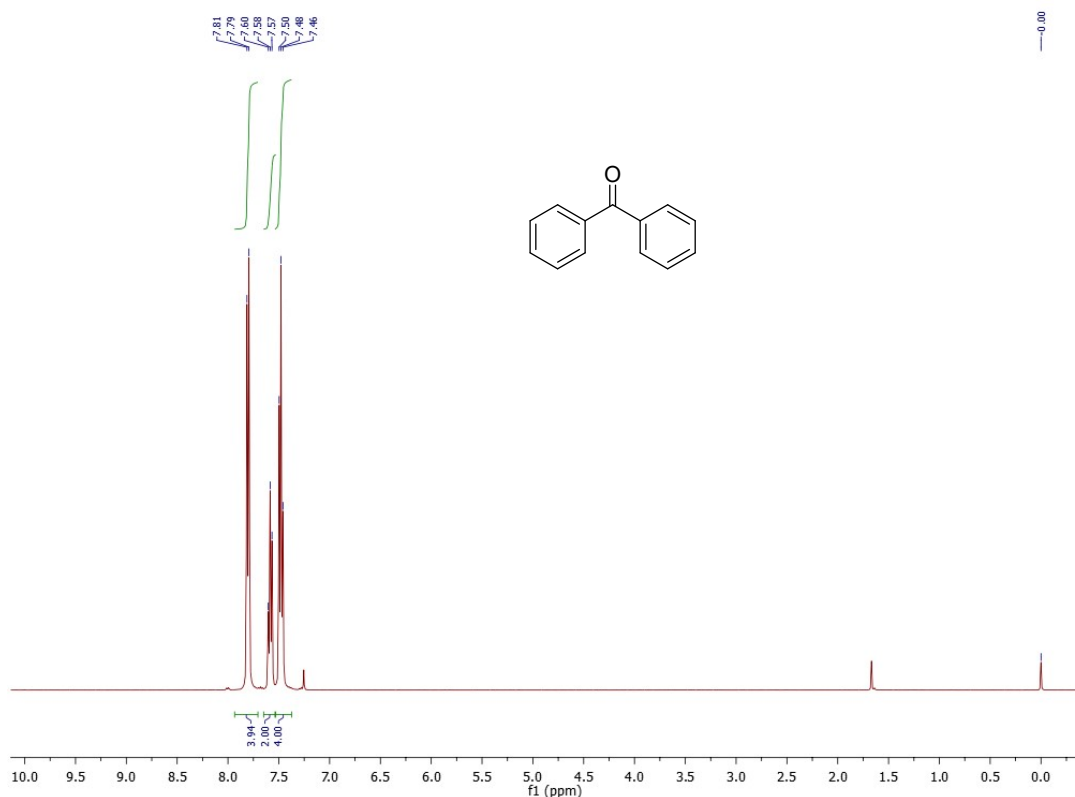


¹³C NMR spectrum of 2g

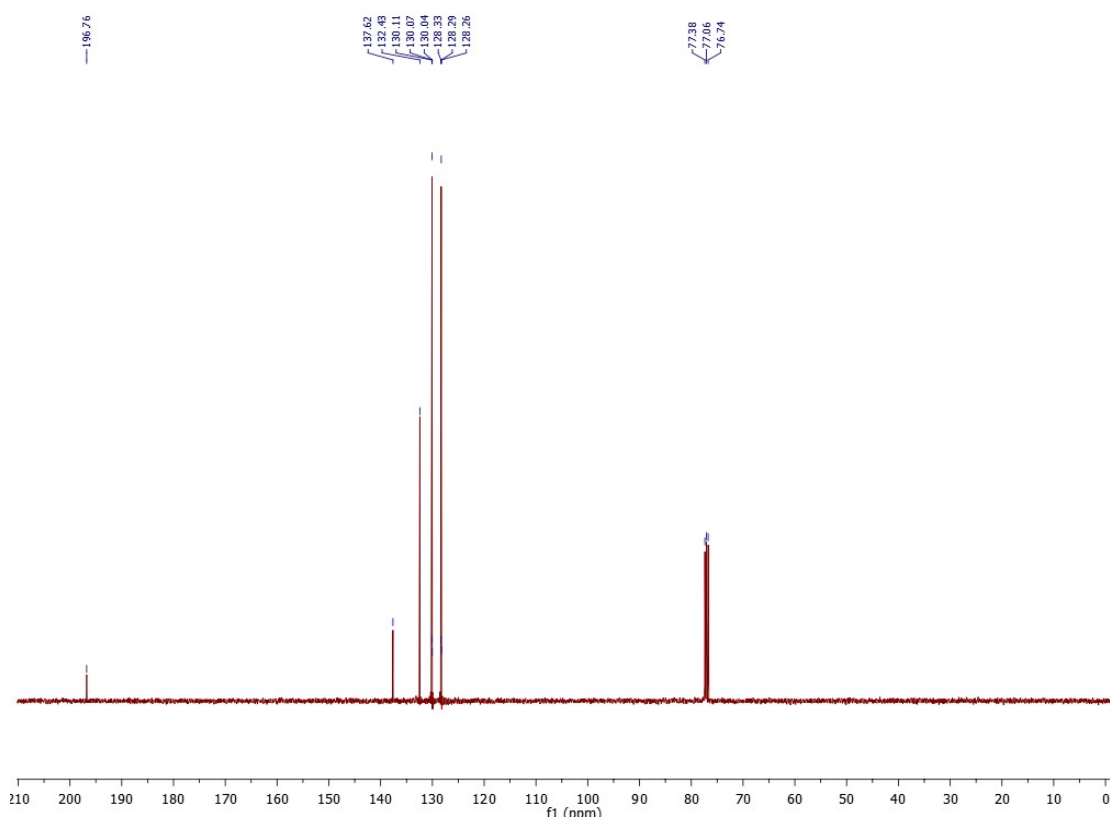
4-Bromo pyridyl methyl ketone (2h)



Benzophenone (2i)

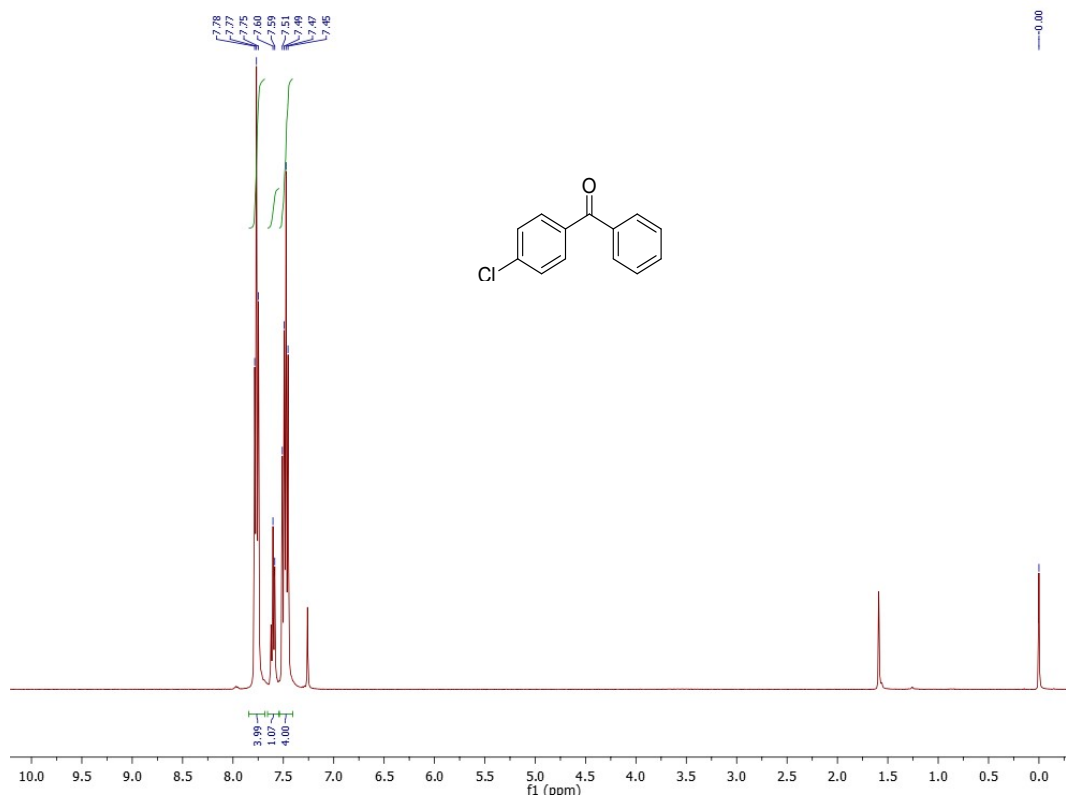


¹H NMR spectrum of **2i**

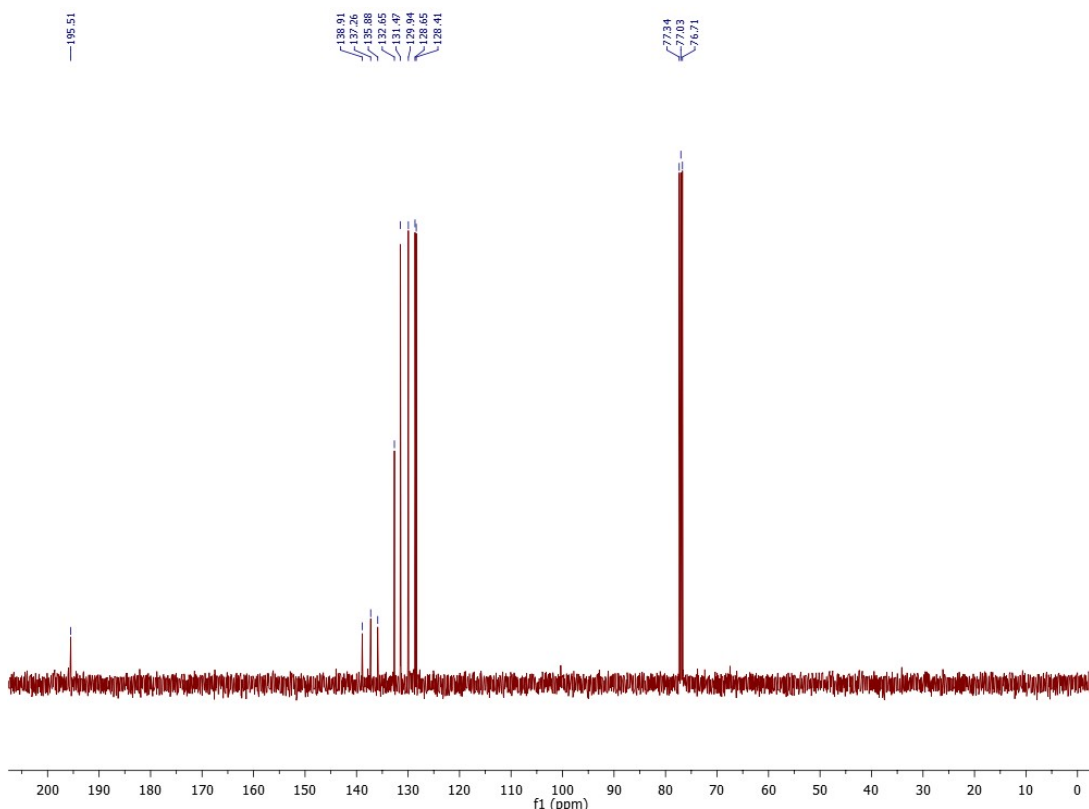


¹³C NMR spectrum of **2i**

4-Chlorobenzophenone(2j)

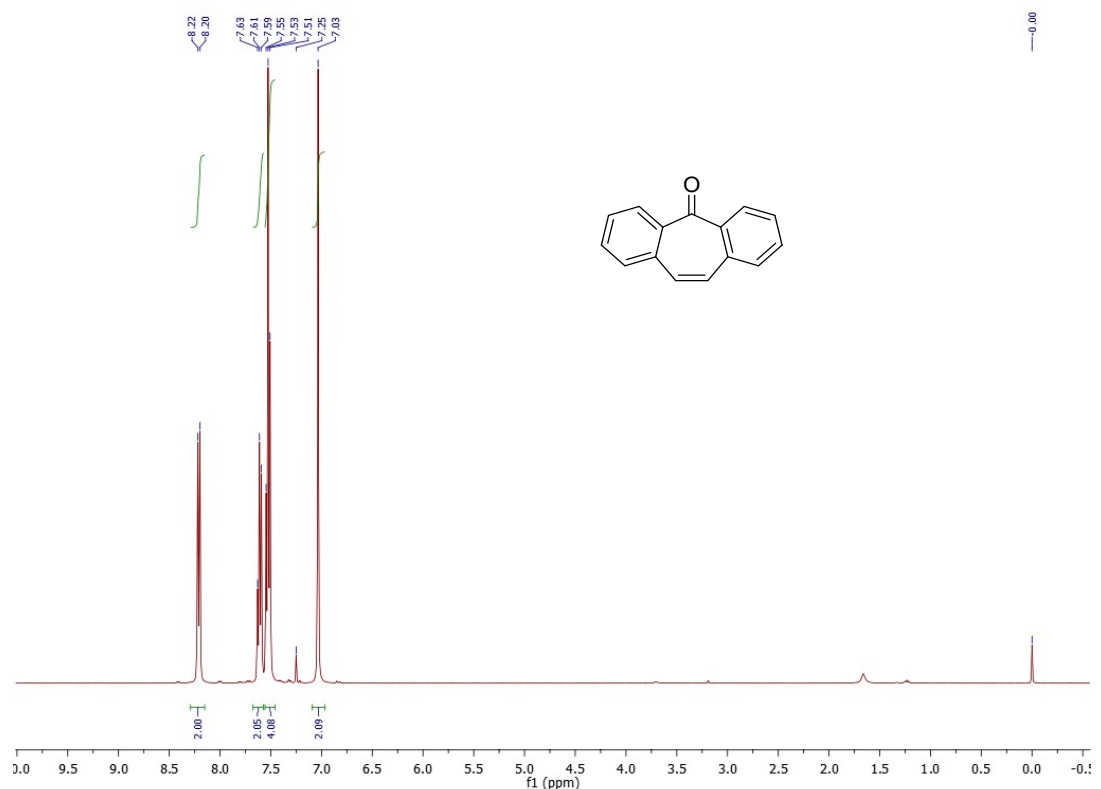


¹H NMR spectrum of **2j**

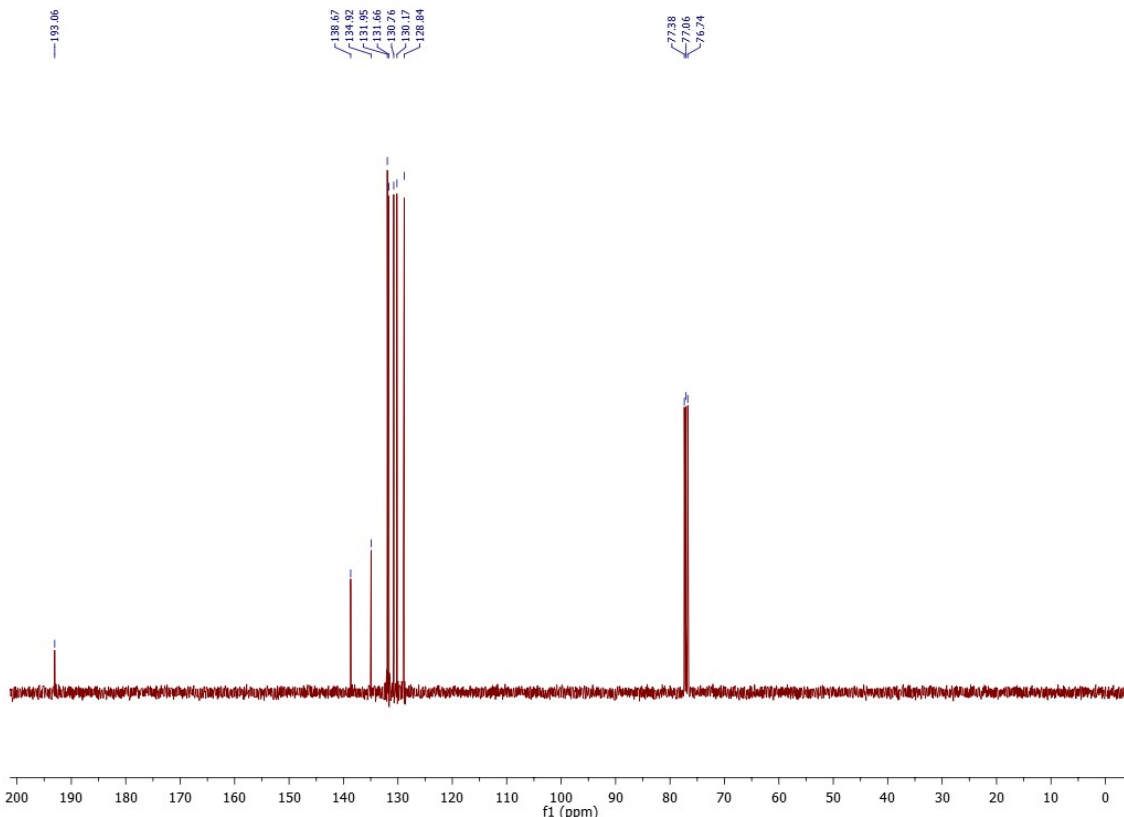


¹³C NMR spectrum of **2j**

Dibenzosuberone (2k)

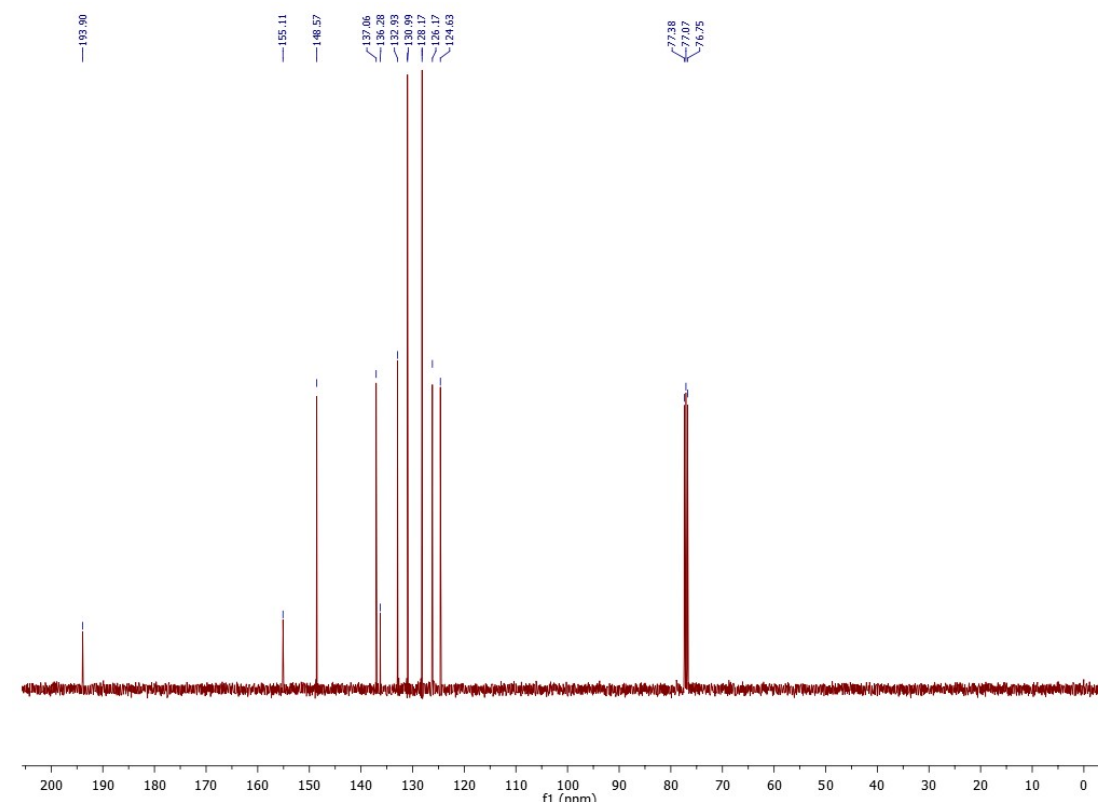
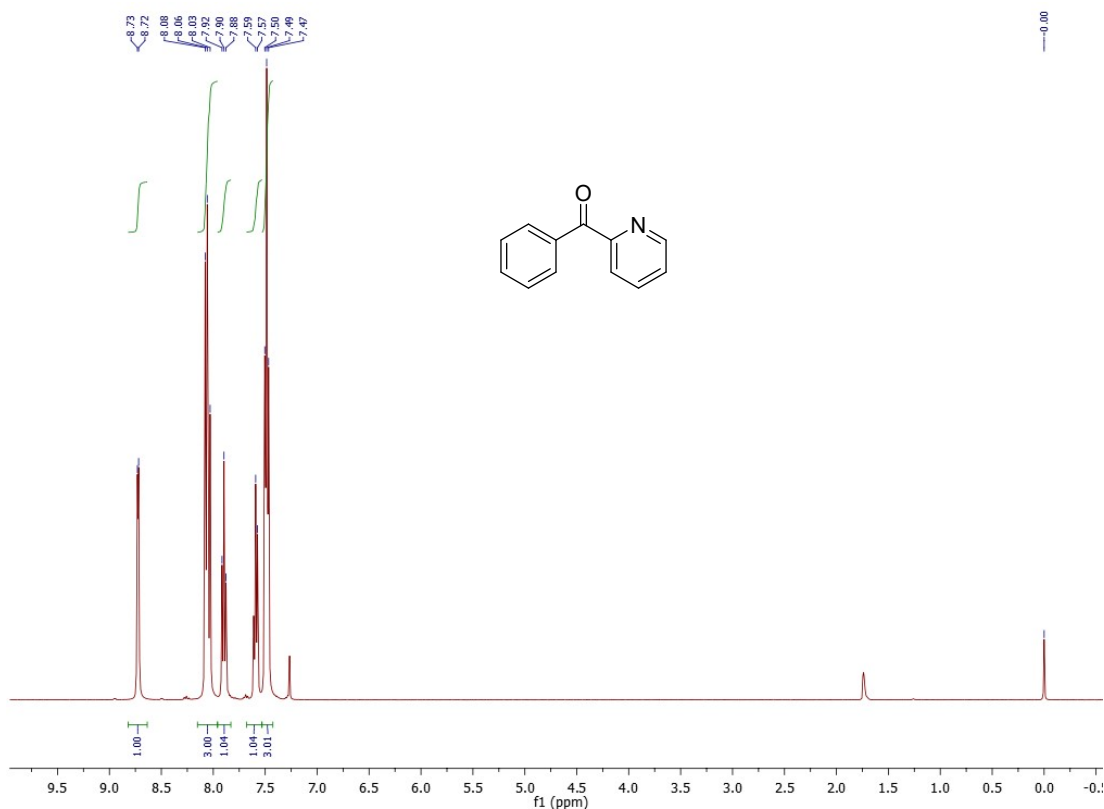


¹H NMR spectrum of **2k**



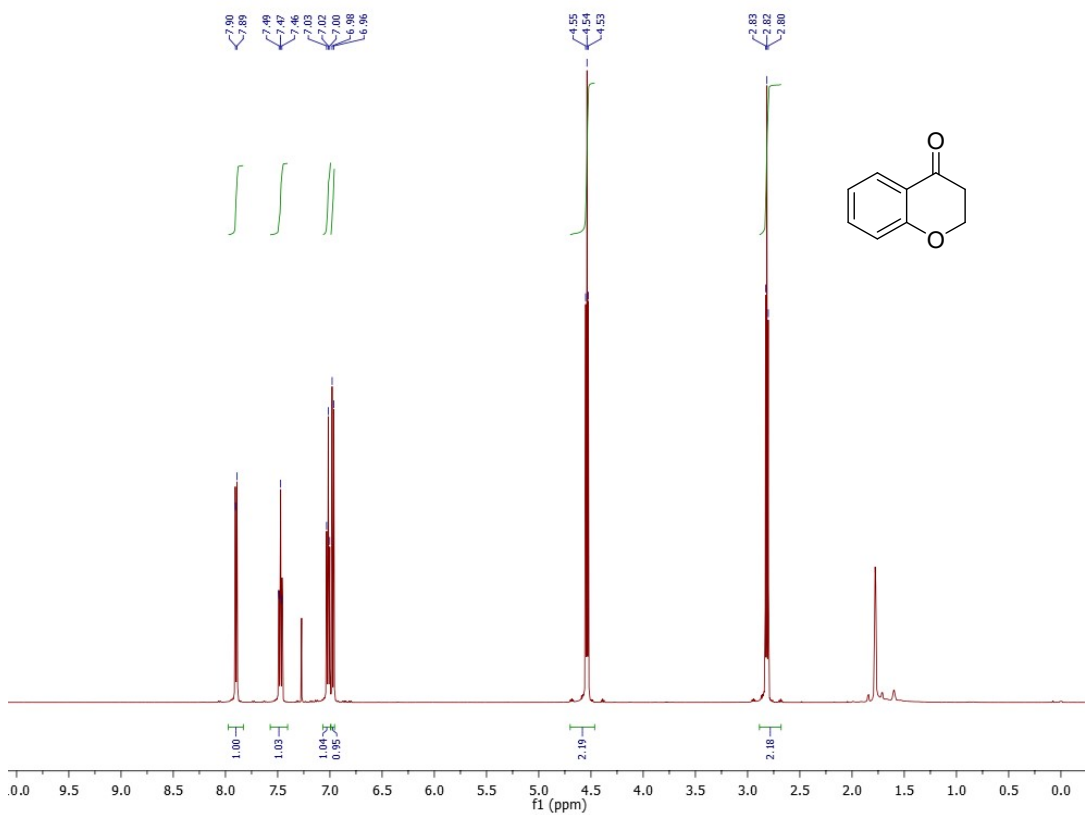
¹³C NMR spectrum of **2k**

Pyridyl acetophenone (2l**)**

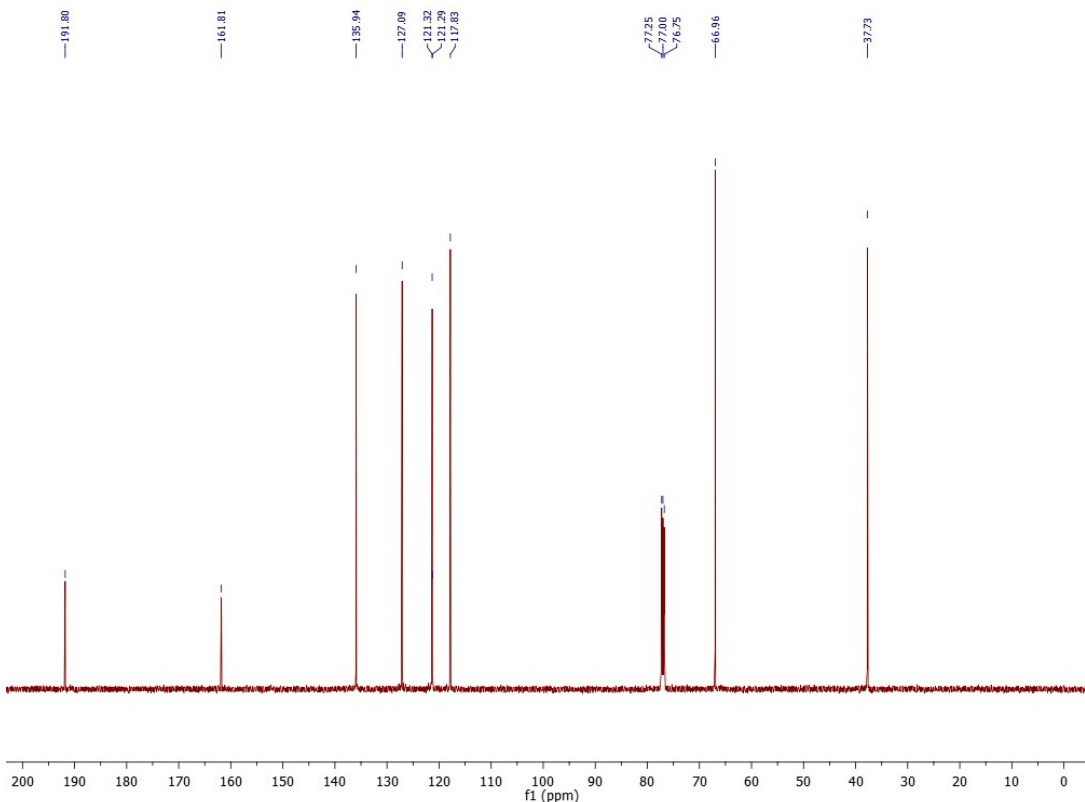


¹³C NMR spectrum of **2l**

Chromone (2m)

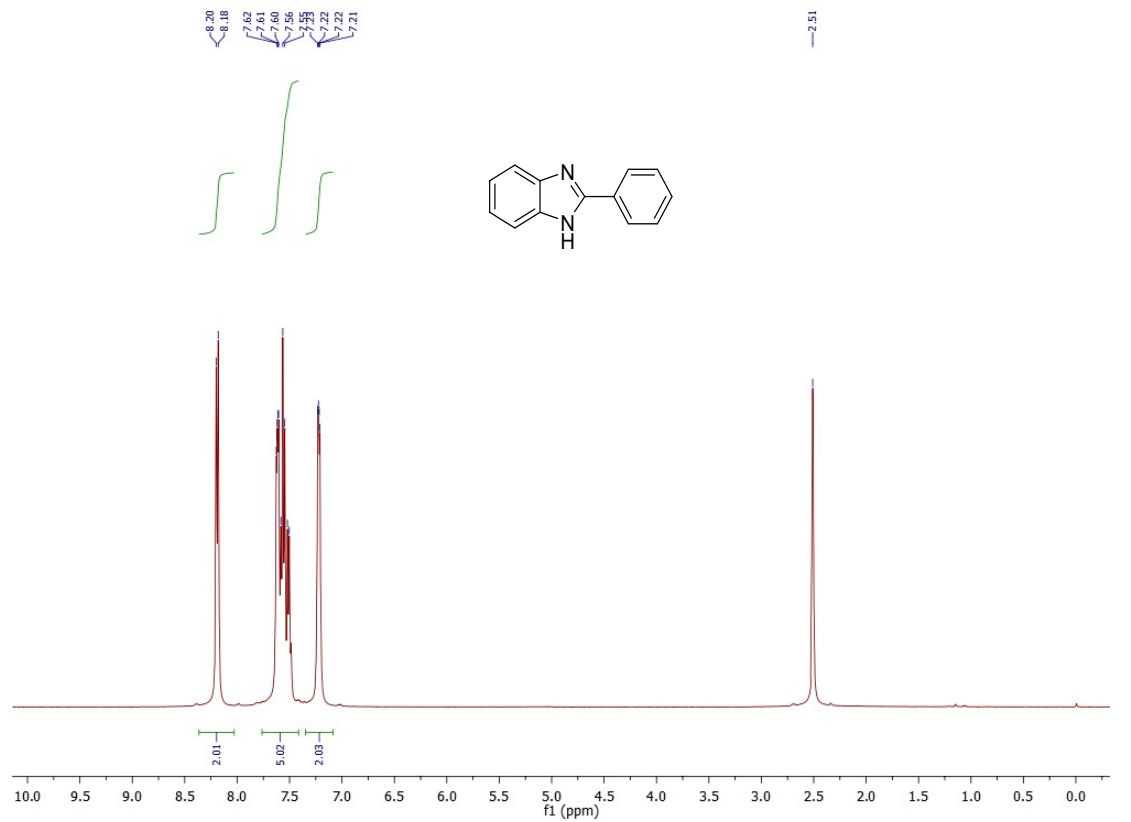


¹H NMR spectrum of **2m**

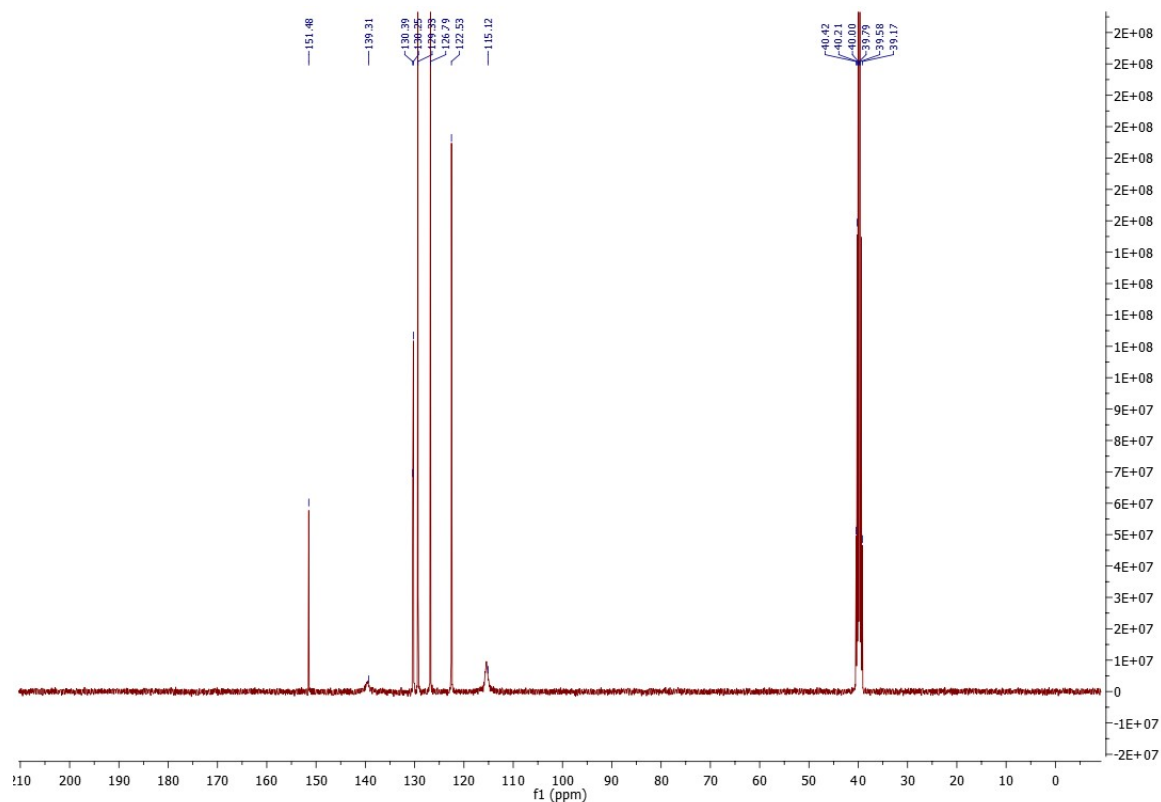


¹³C NMR spectrum of **2m**

2-Phenyl-1H-benzo[d]imidazole (6a)

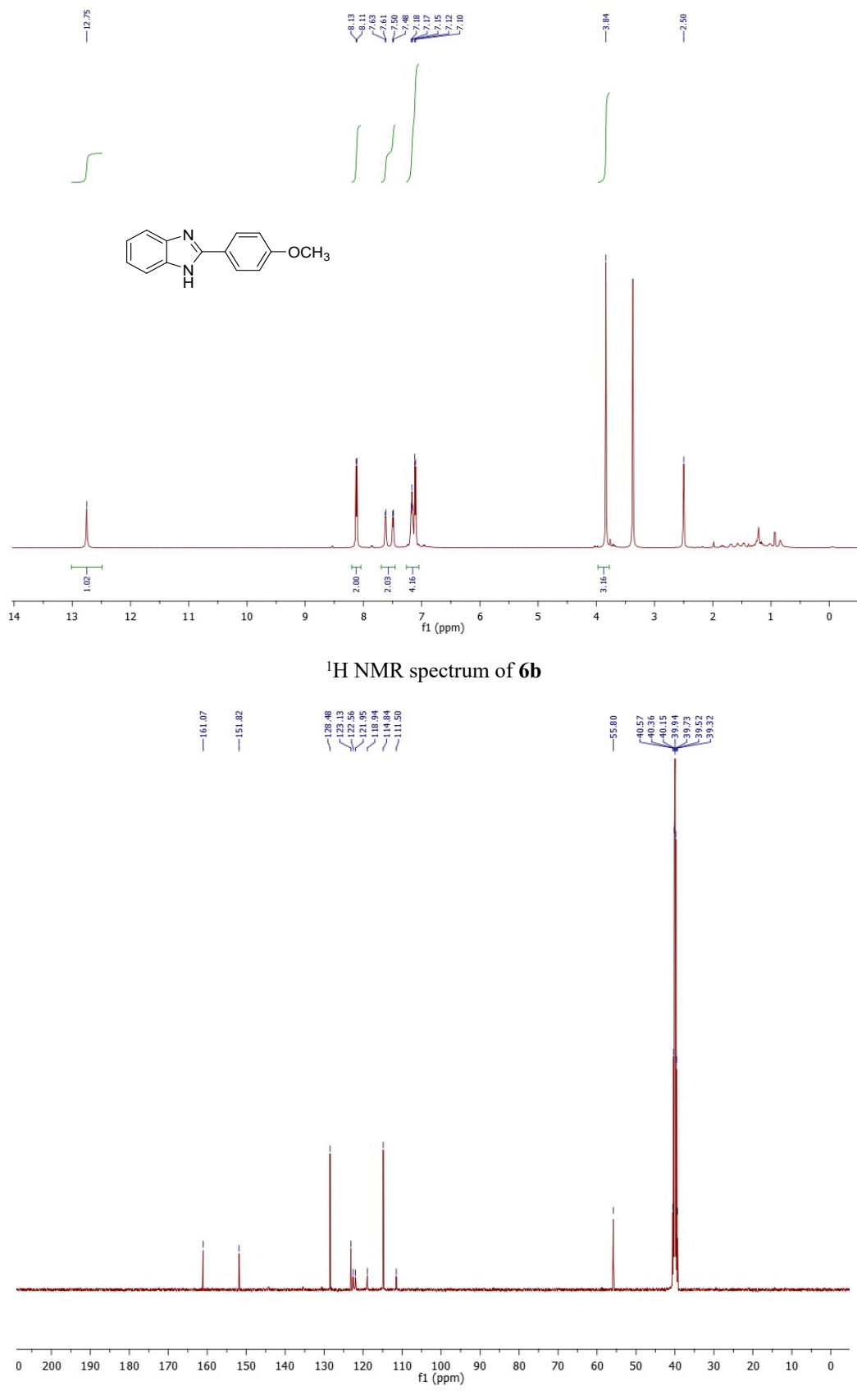


¹H NMR spectrum of 6a



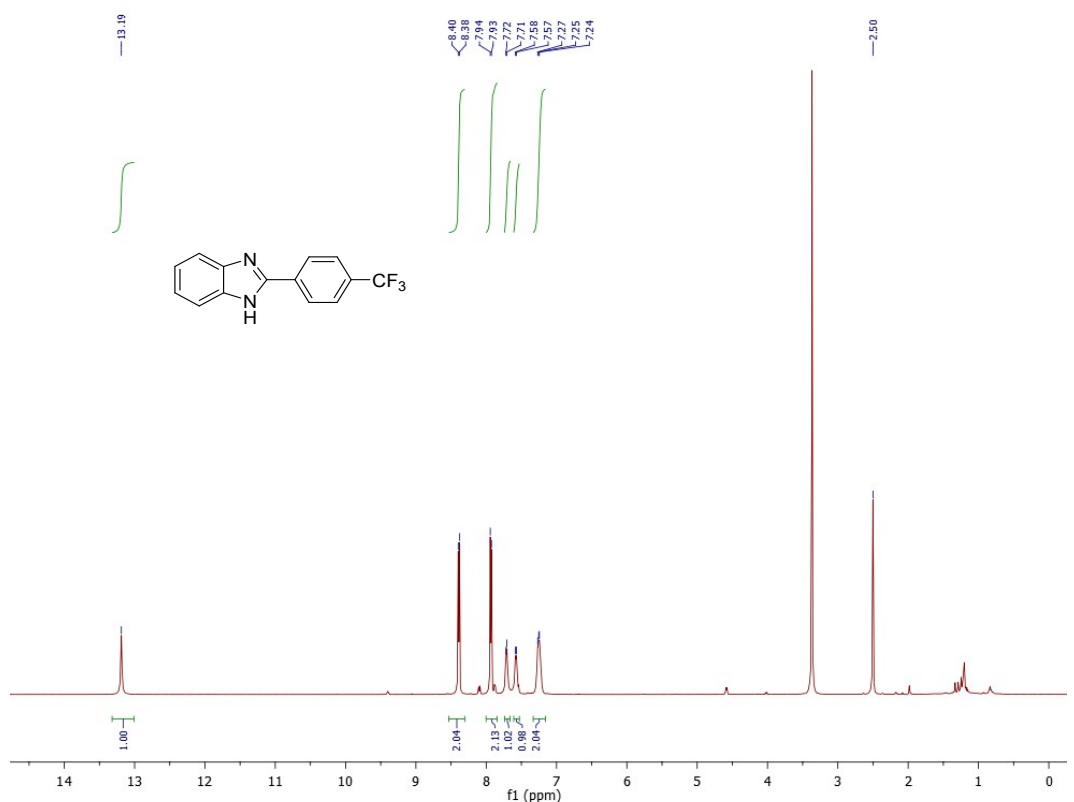
¹³C NMR spectrum of 6a

2-(4-Methoxyphenyl)-1H-benzo[d]imidazole (6b)

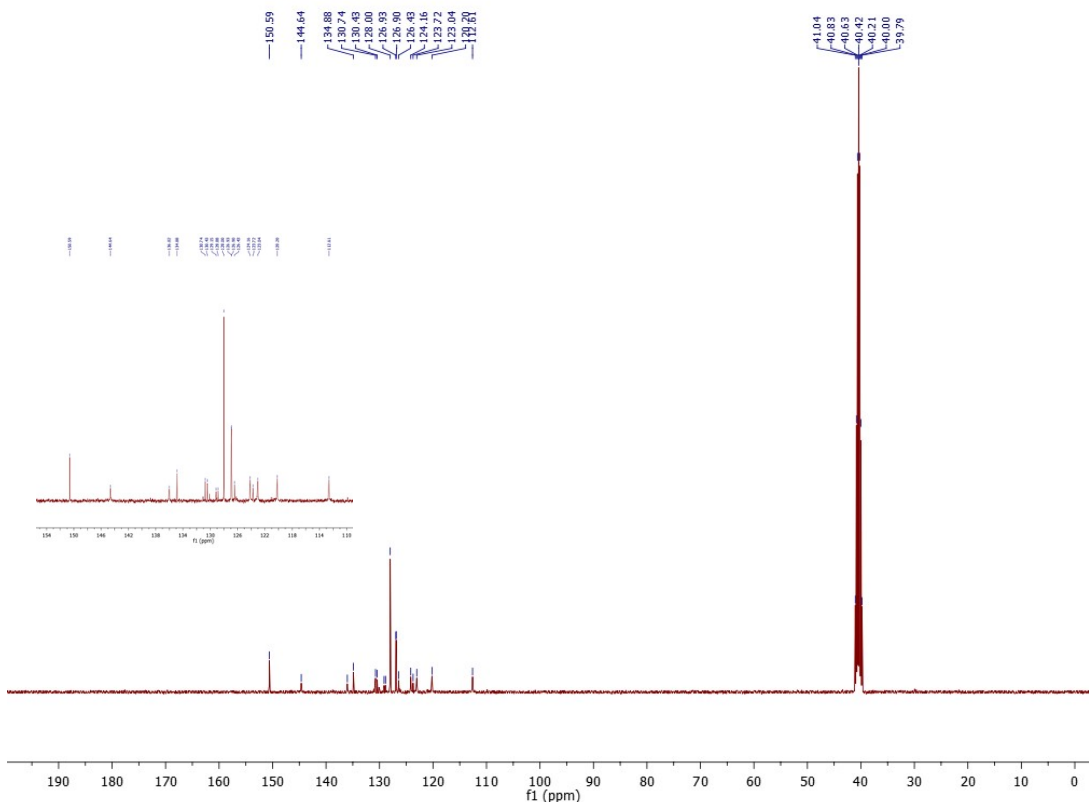


¹³C NMR spectrum of 6b

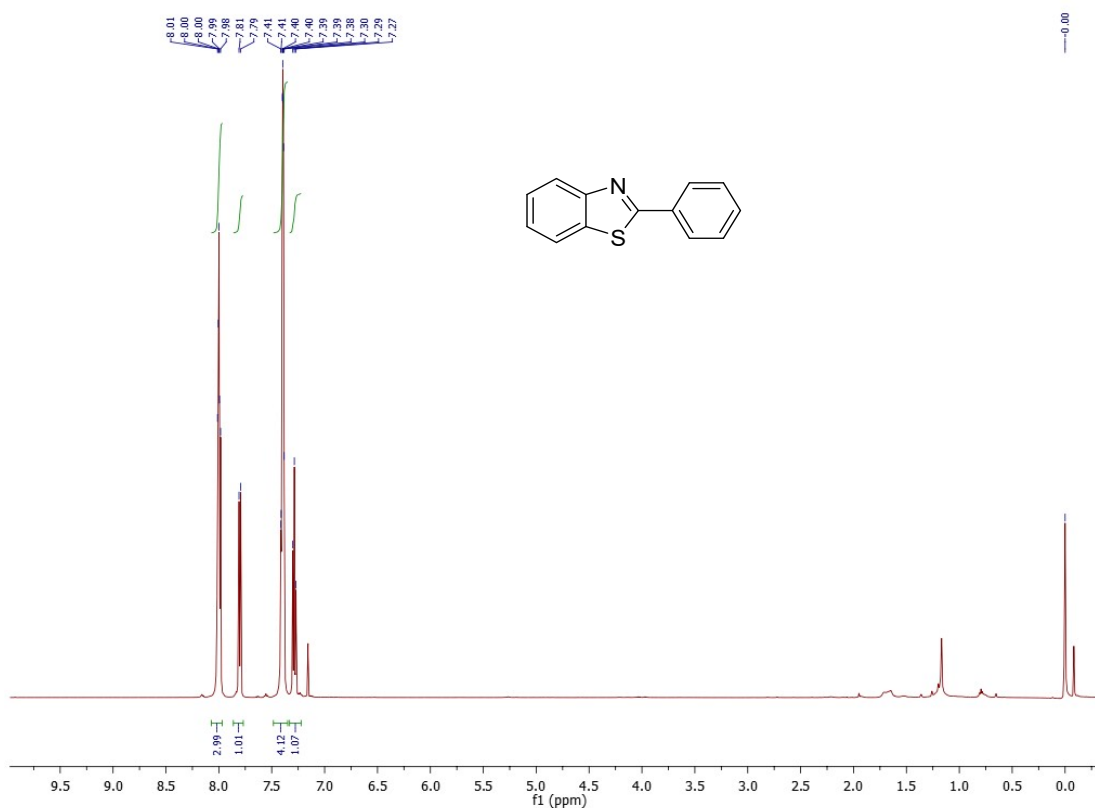
2-(4-(Trifluoromethyl) phenyl)-1H-benzo[d]imidazole (6c)



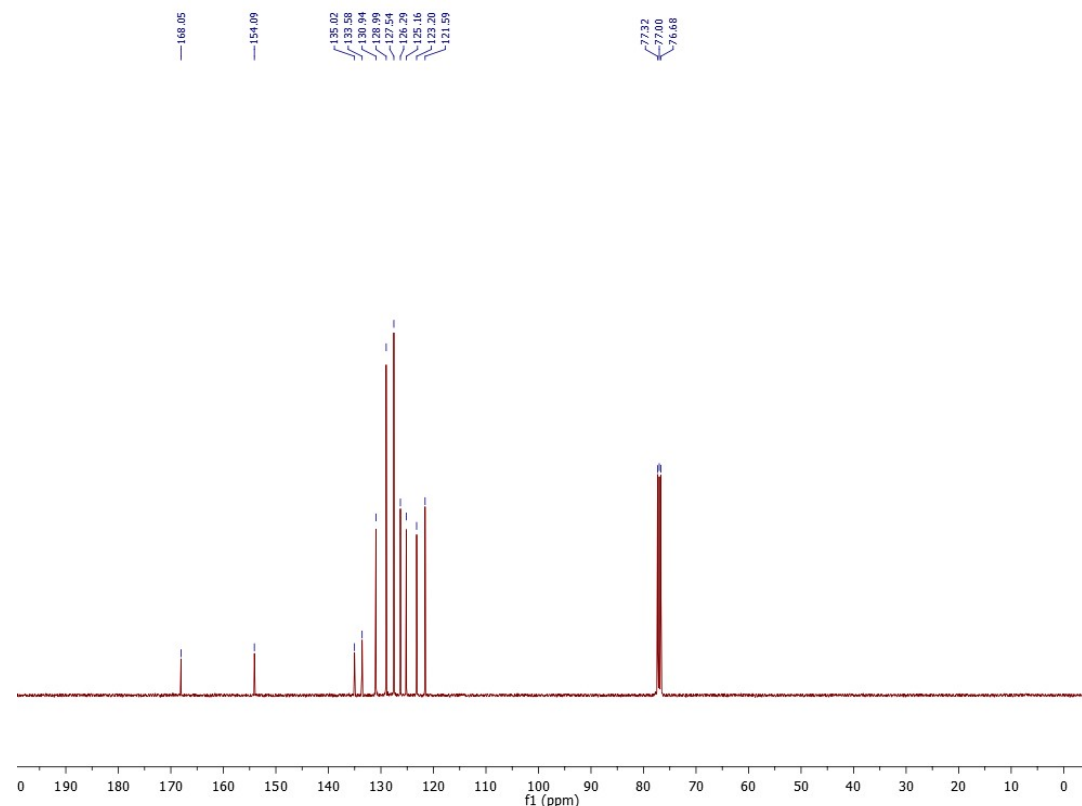
¹H NMR spectrum of 6c



2-Phenylbenzothiazole(6d)

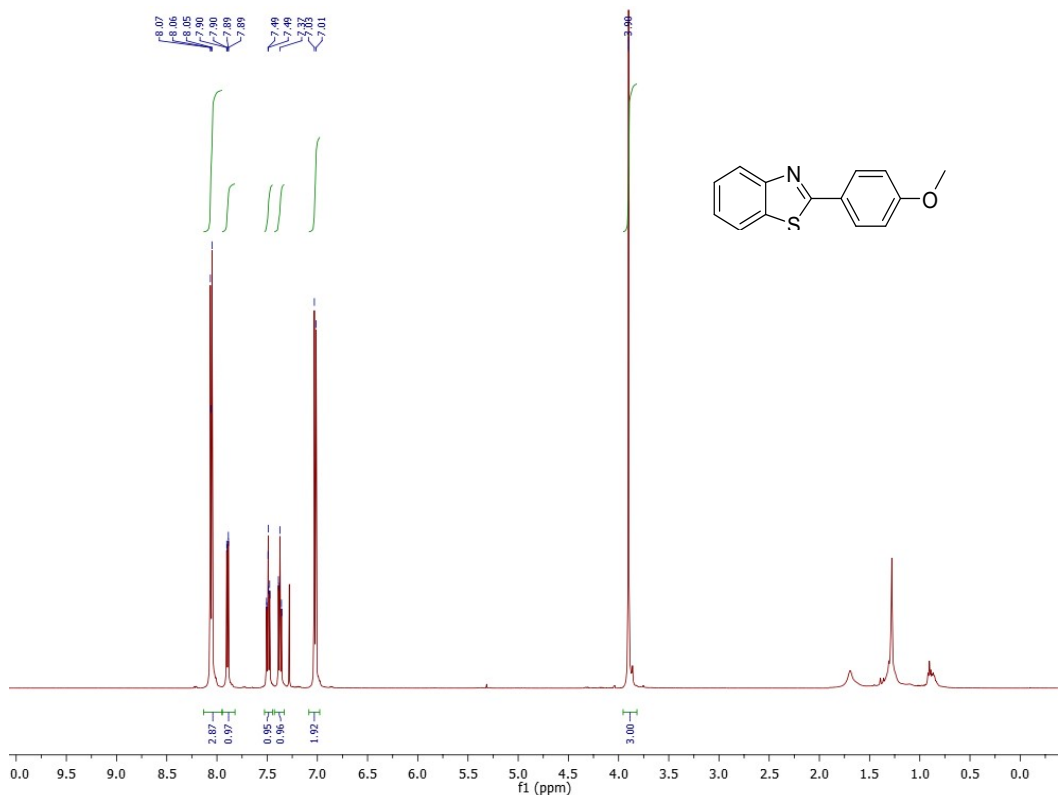


¹H NMR spectrum of **6d**

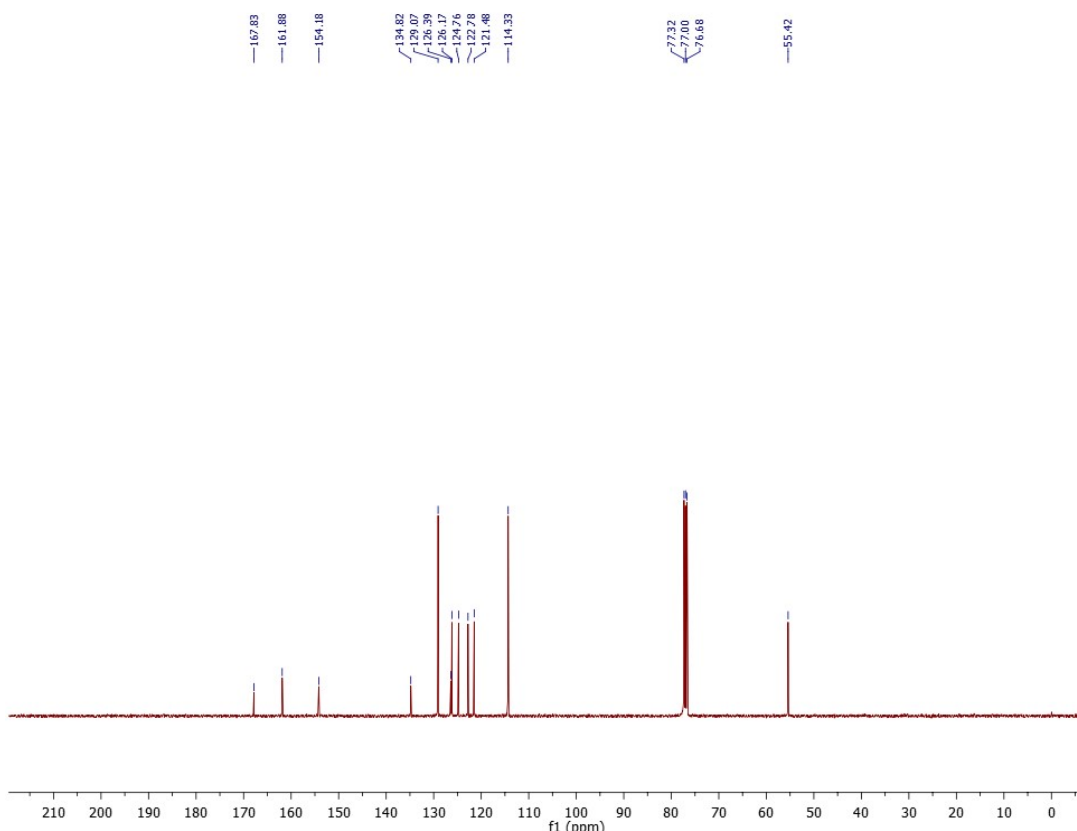


¹³C NMR spectrum of **6d**

2-(4-Methoxyphenyl)benzothiazole(6e)

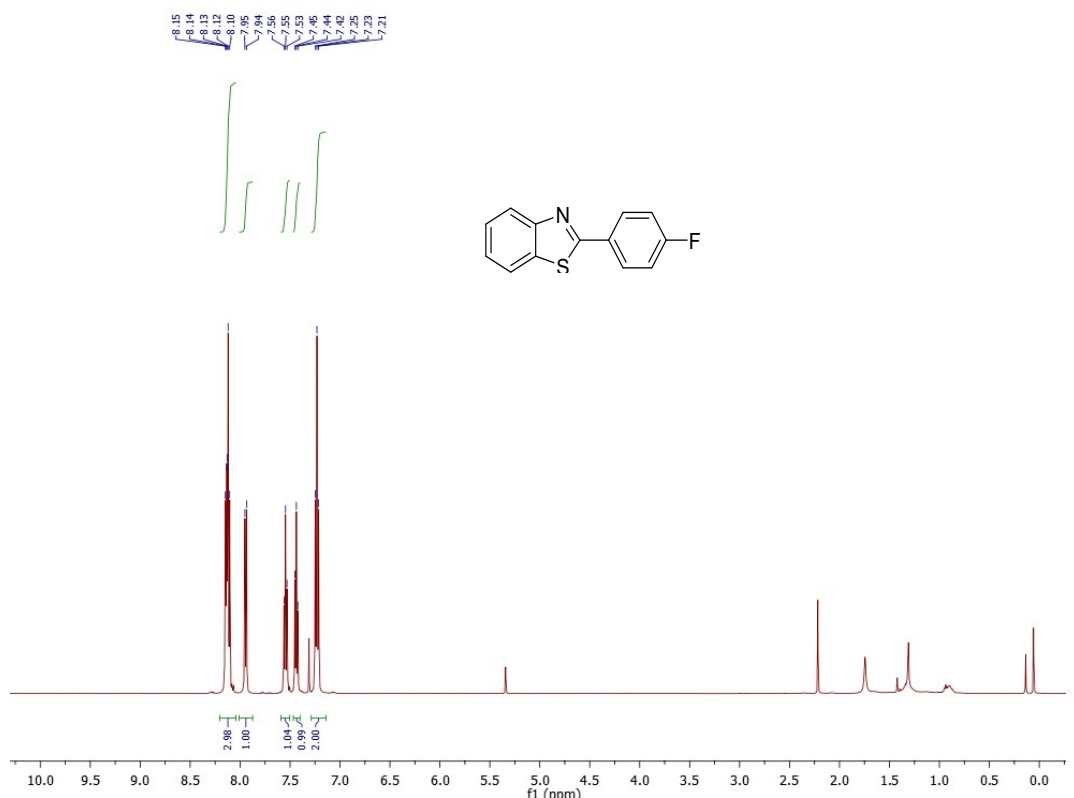


¹H NMR spectrum of **6e**

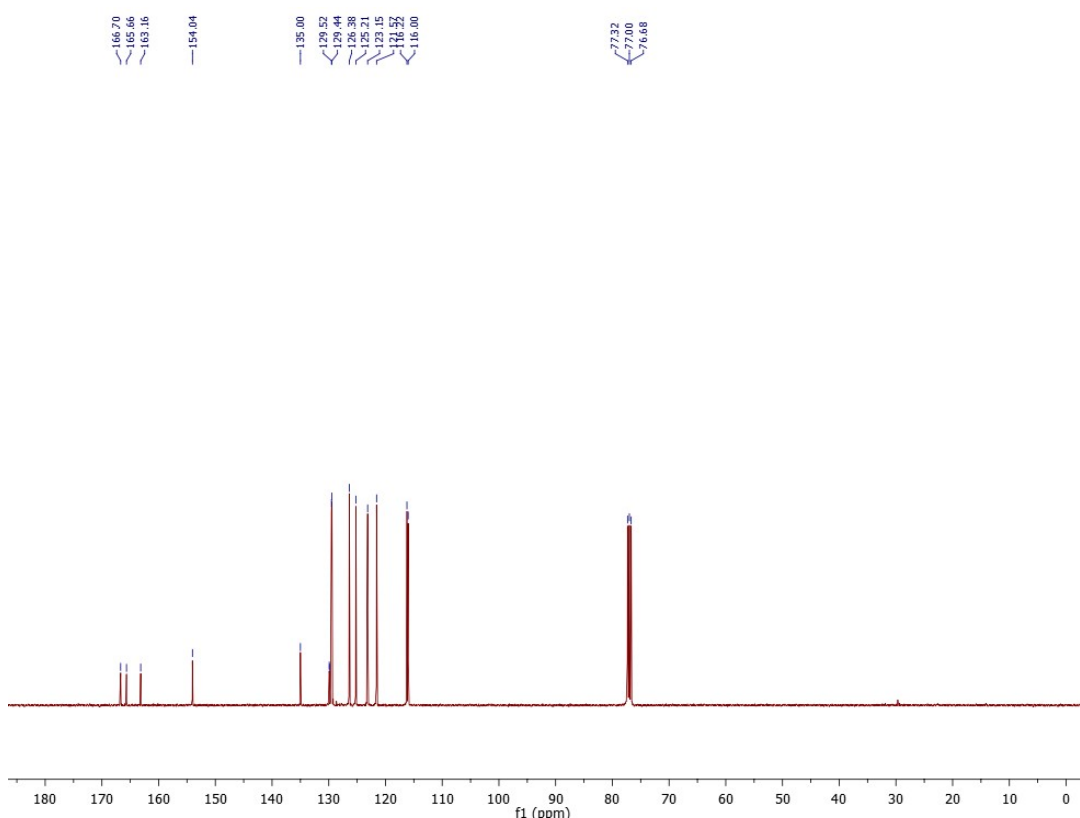


¹³C NMR spectrum of **6e**

2-(4-Fluorophenyl)benzothiazole(6f)

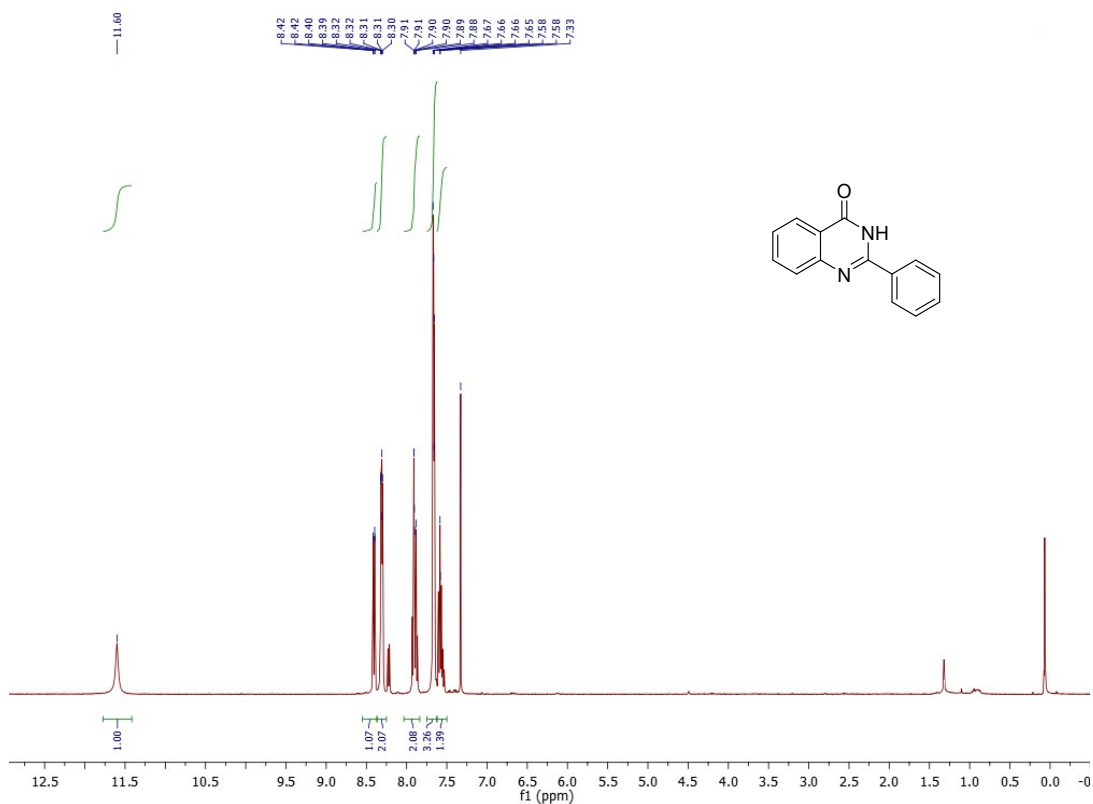


¹H NMR spectrum of **6f**

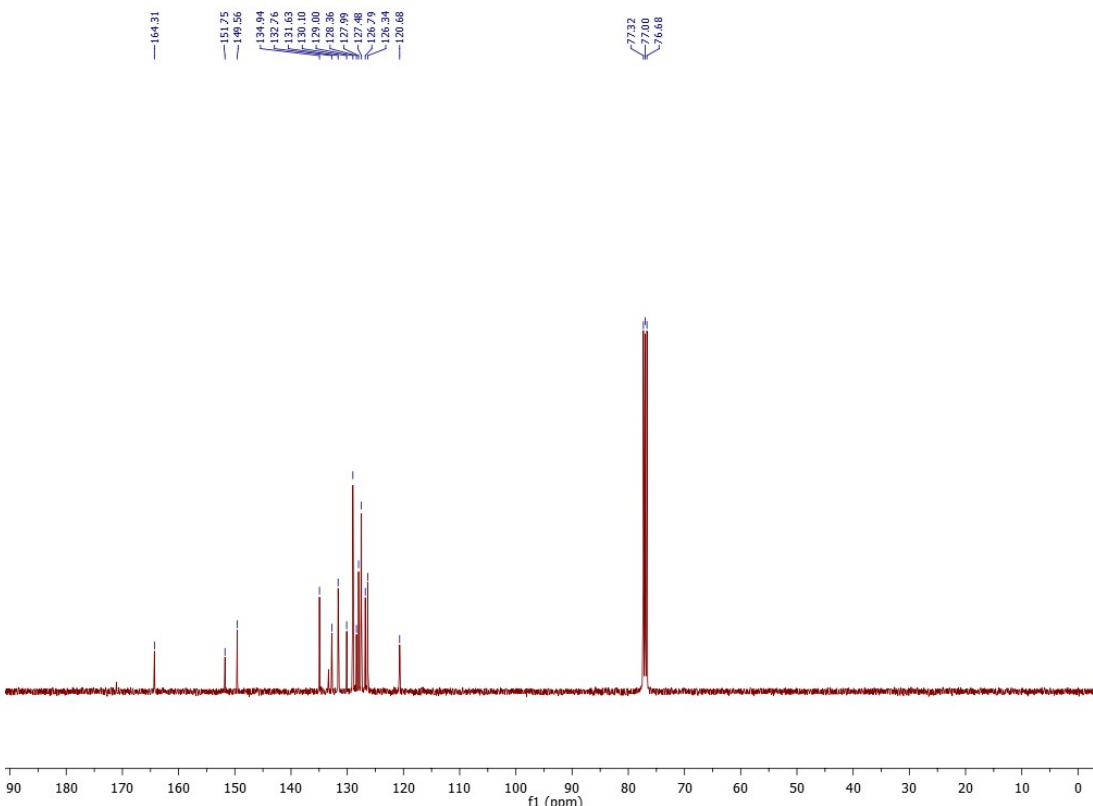


¹³C NMR spectrum of **6f**

2-Phenylquinazolin-4(3H)-one (6g)

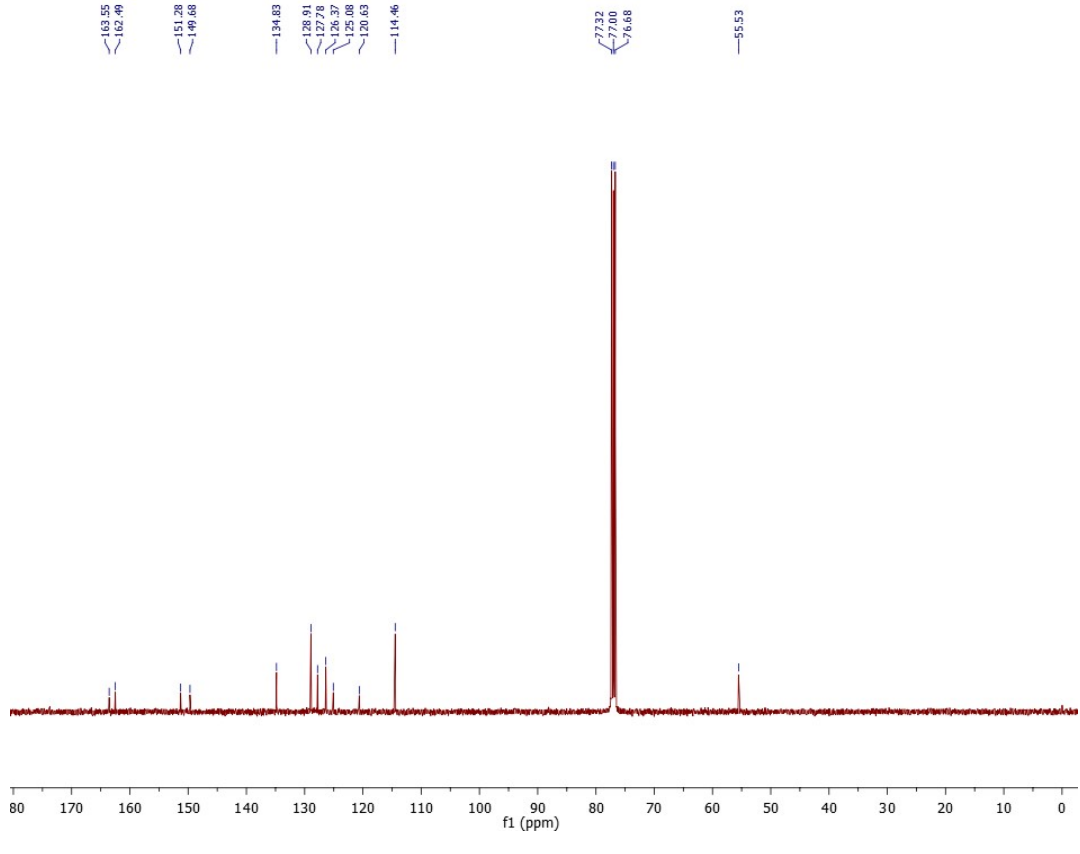
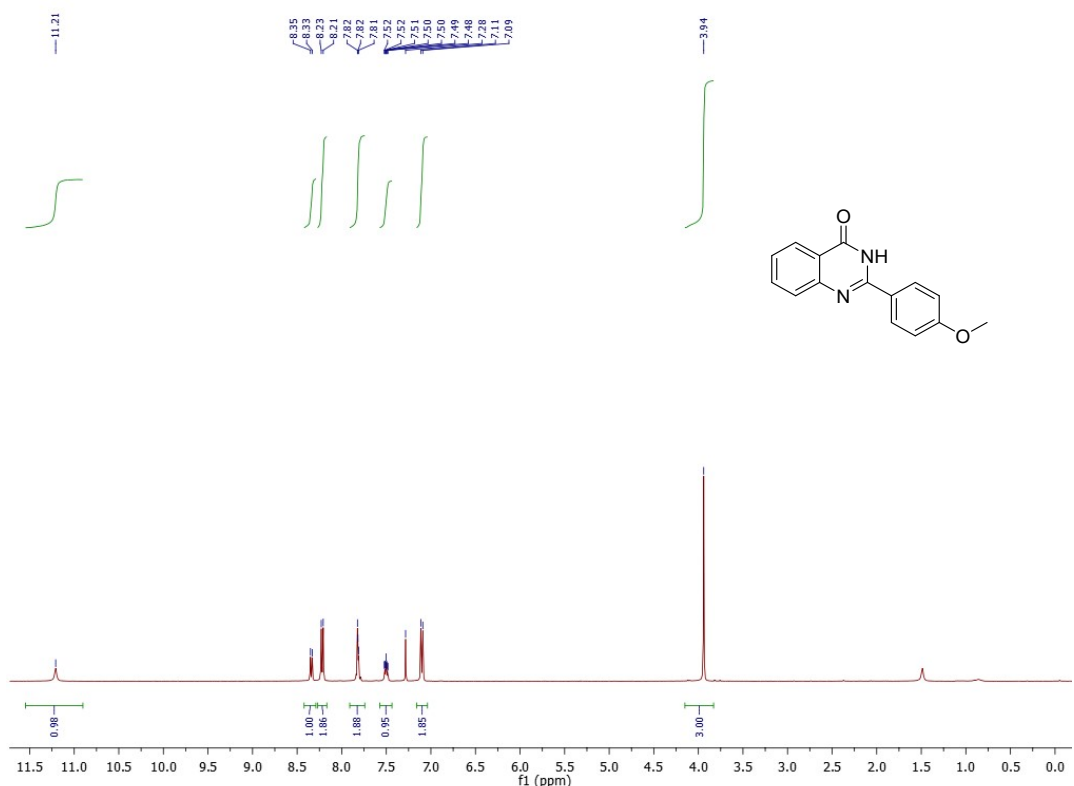


¹H NMR spectrum of **6g**

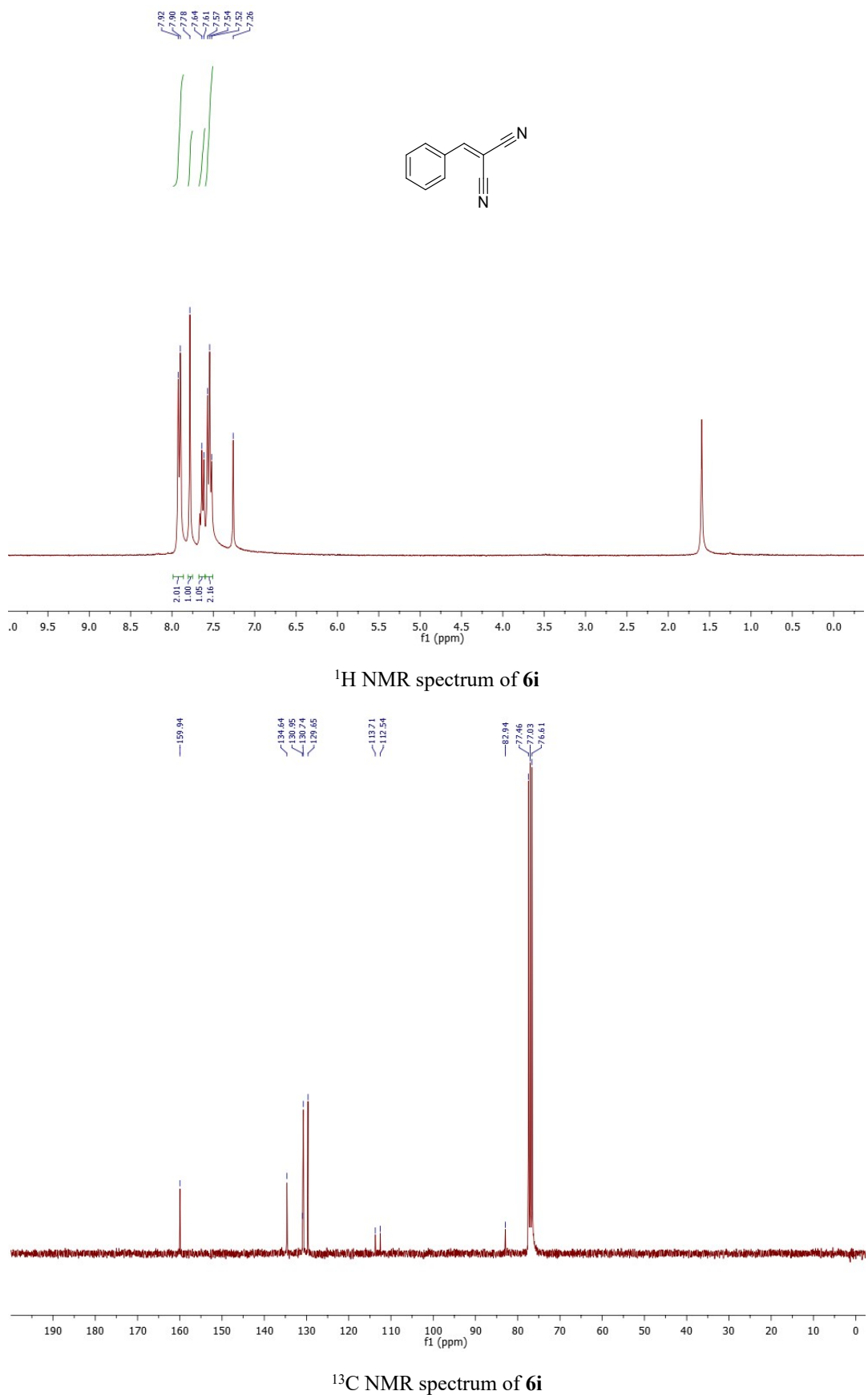


¹³C NMR spectrum of **6g**

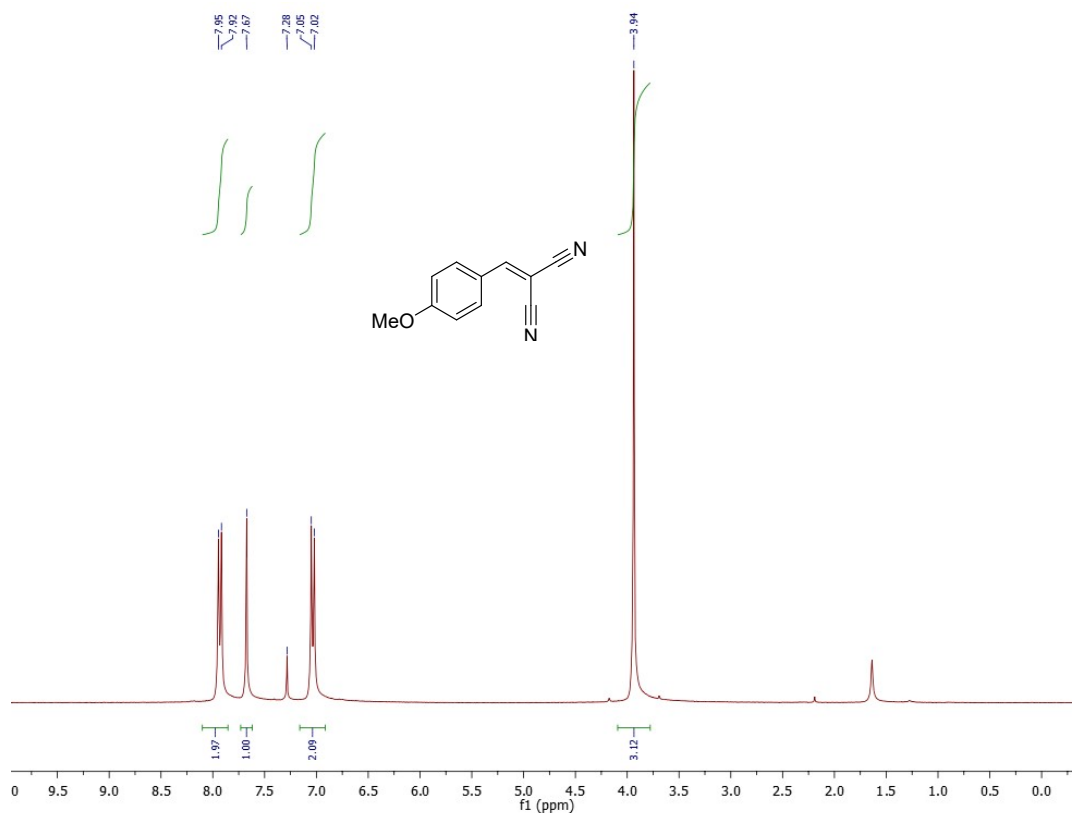
2-(4-Methoxyphenyl)quinazolin-4(3*H*)-one (6h**)**



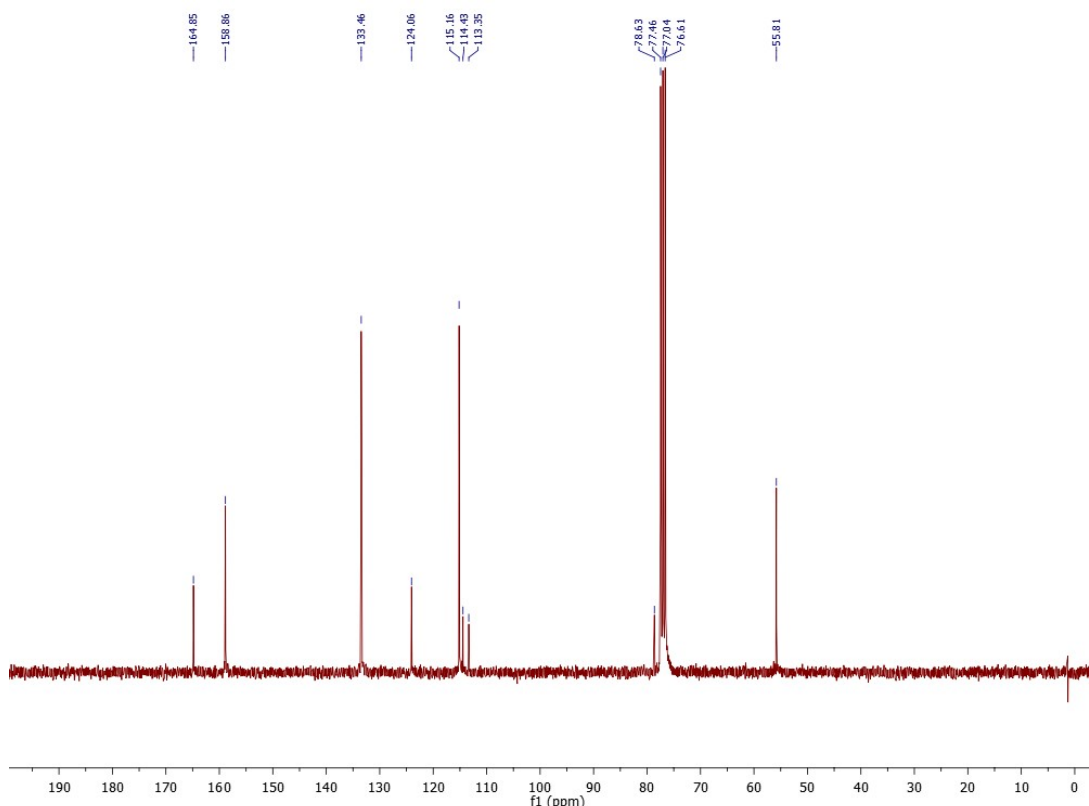
2-Benzylidene malononitrile (6i)



2-(4-Methoxybenzylidene)malononitrile (6j)

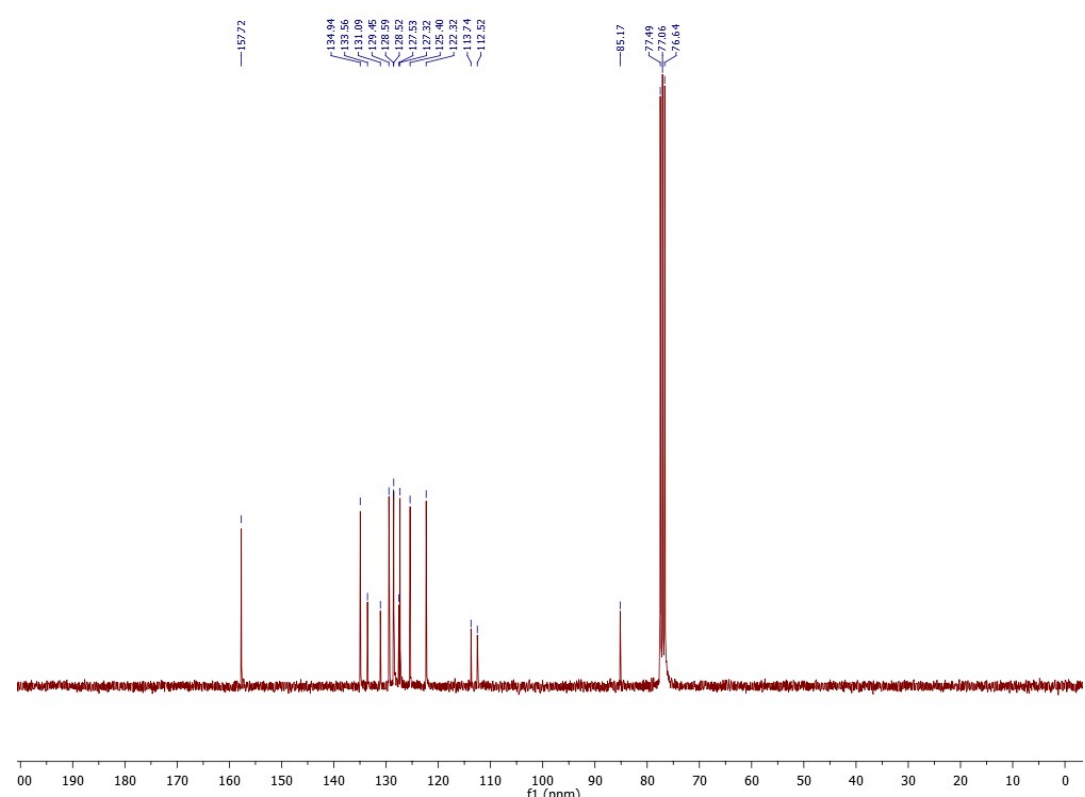
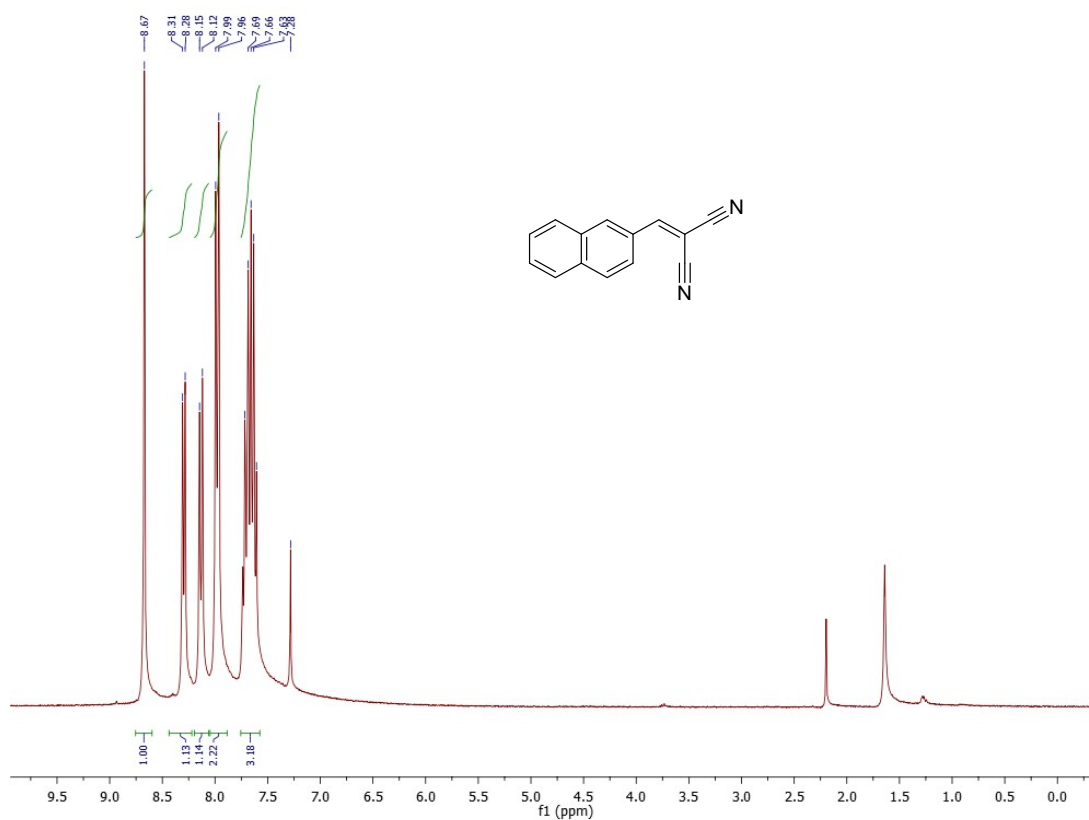


¹H NMR spectrum of **6j**



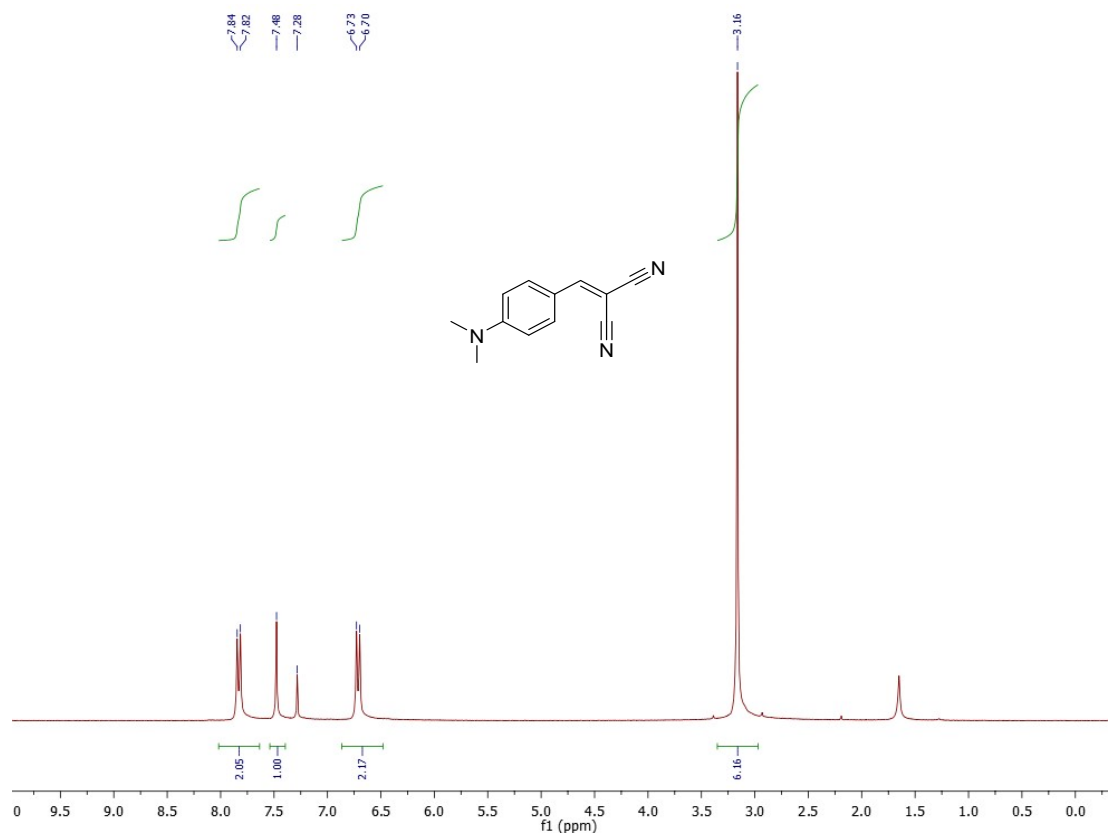
¹³C NMR spectrum of **6j**

2-(Naphthalen-2-ylmethylene)malononitrile (6k**)**

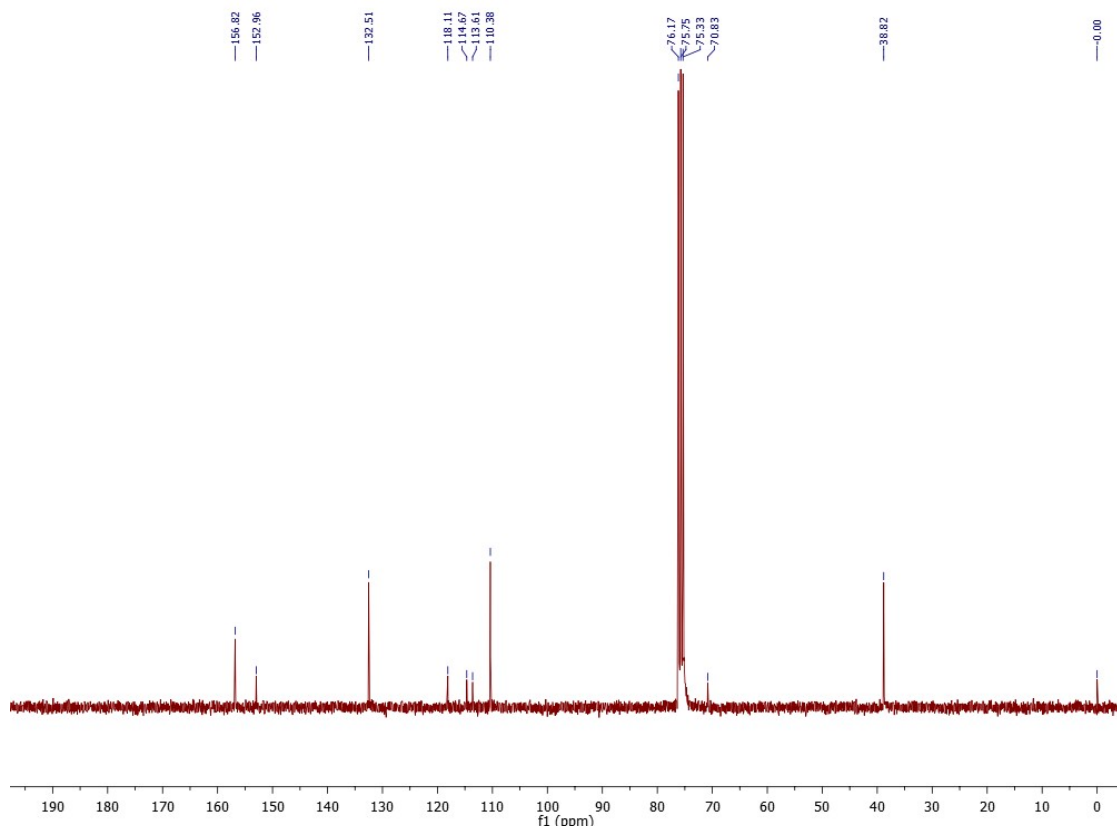


^{13}C NMR spectrum of **6k**

2-(4-(Dimethylamino)benzylidene)malononitrile (6l)

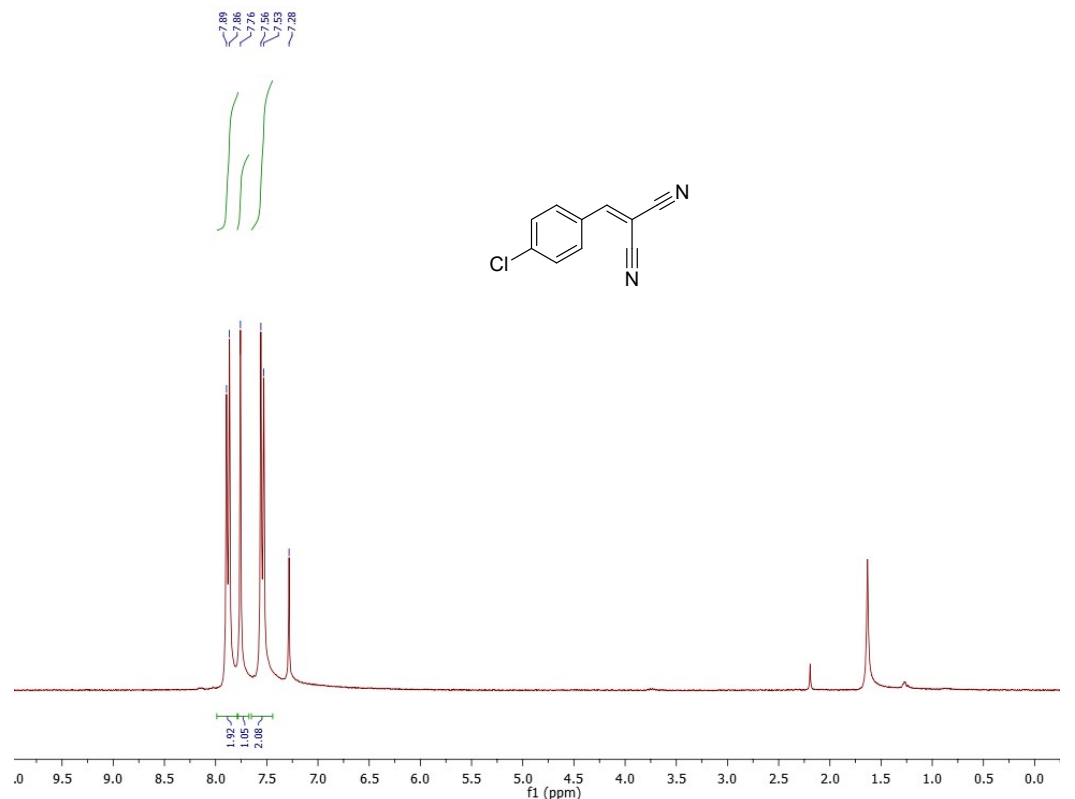


¹H NMR spectrum of **6l**

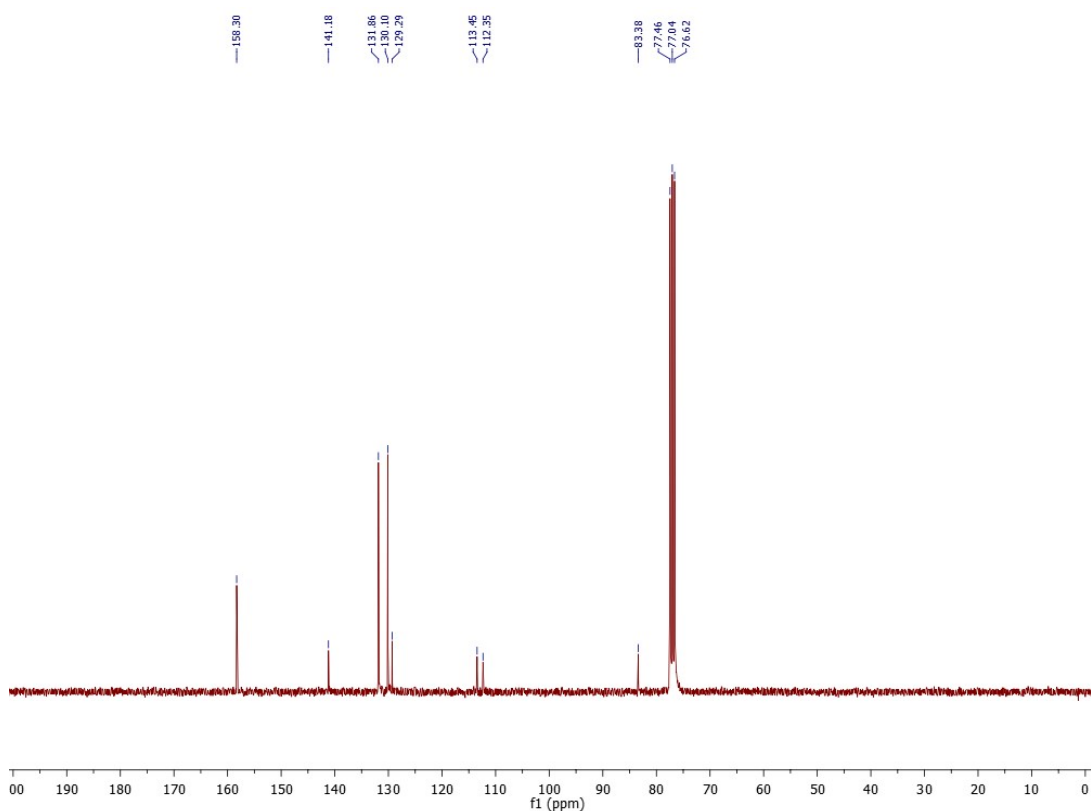


¹³C NMR spectrum of **6l**

2-(4-Chlorobenzylidene)malononitrile (6m)

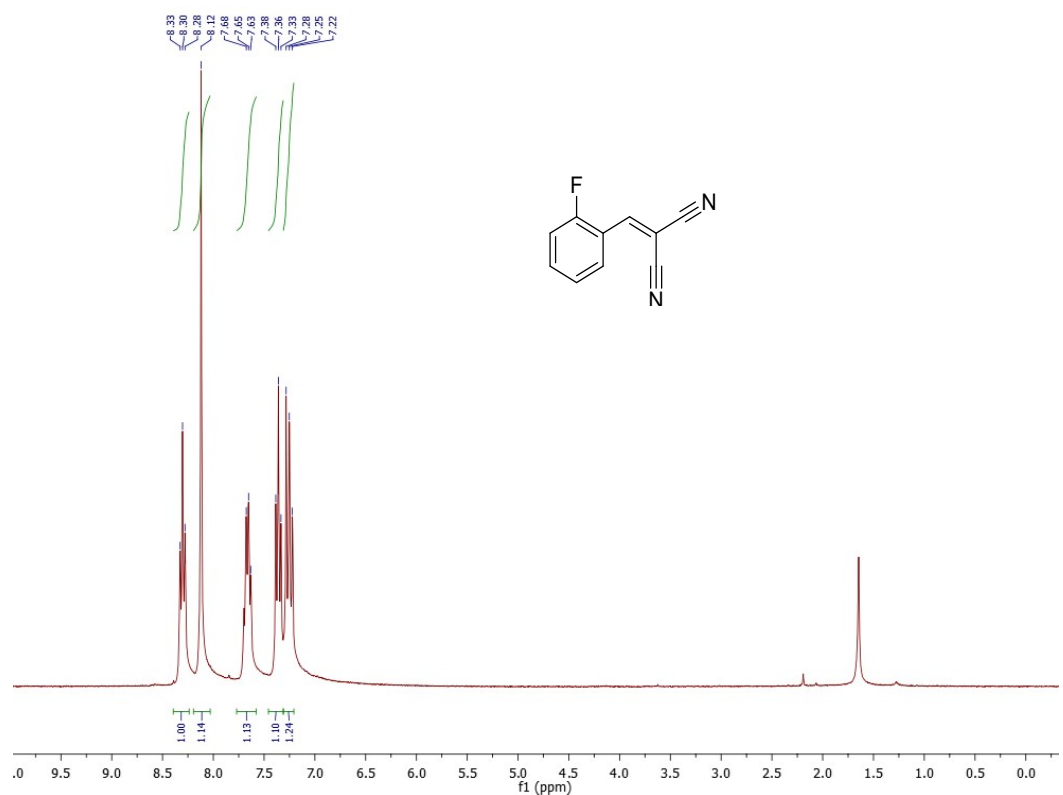


¹H NMR spectrum of **6m**

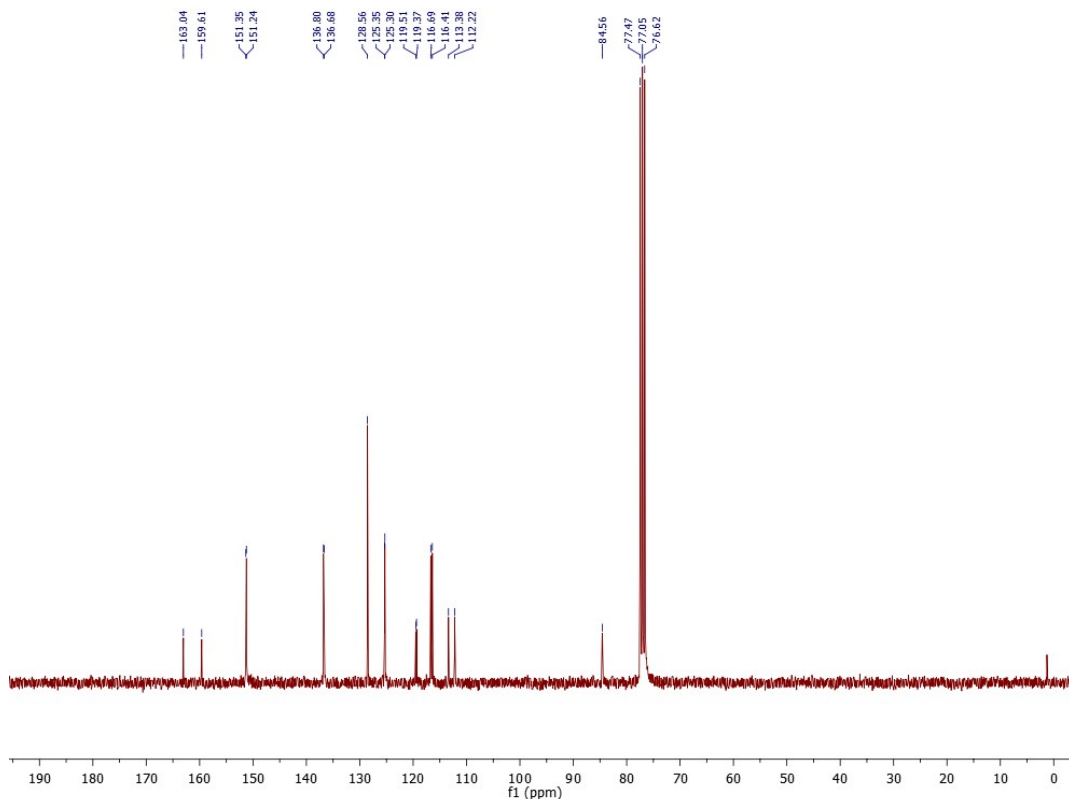


¹³C NMR spectrum of **6m**

2-(2-Fluorobenzylidene)malononitrile (6n)

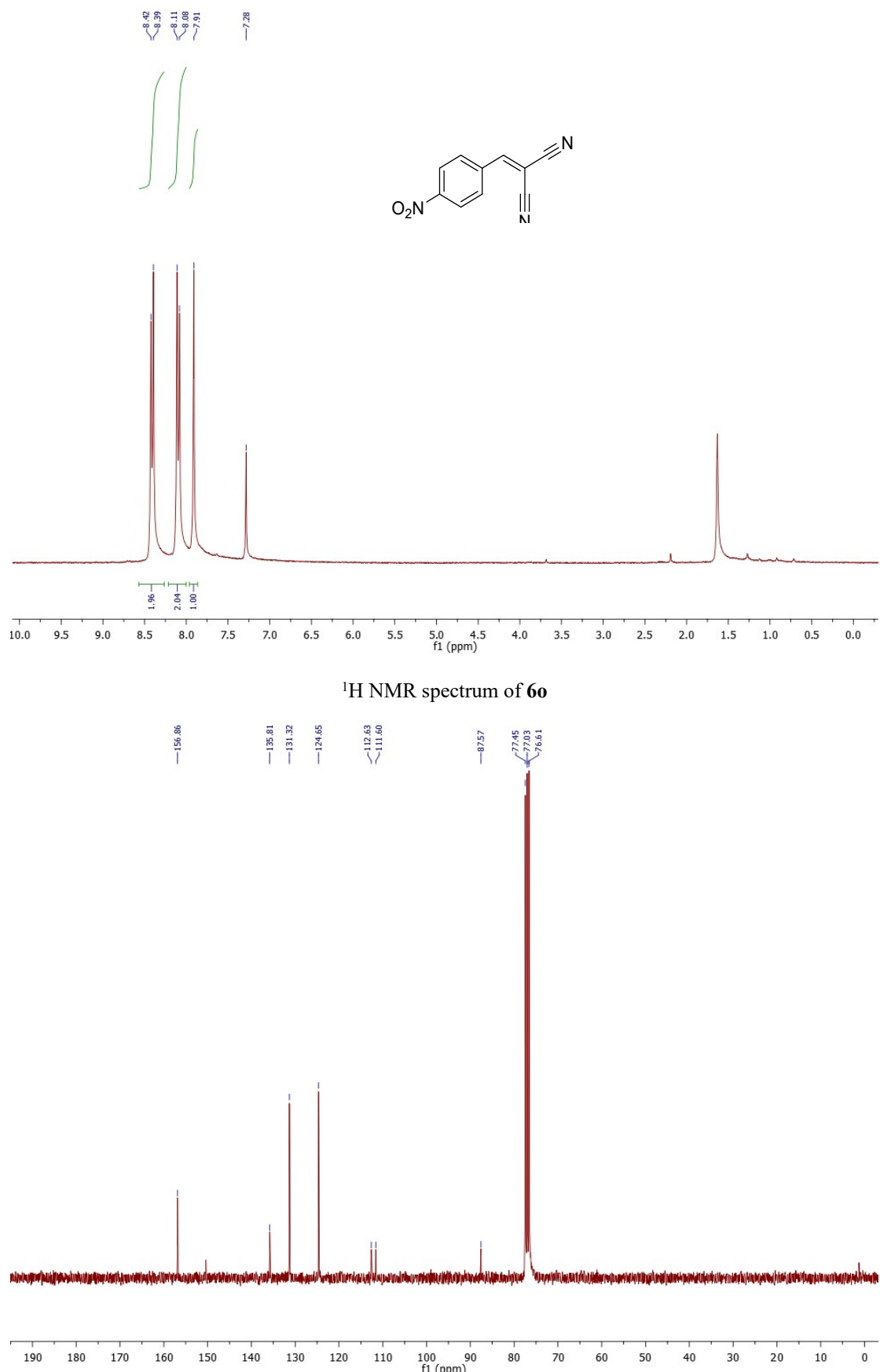


¹H NMR spectrum of 6n



¹³C NMR spectrum of 6n

2-(4-Nitrobenzylidene)malononitrile (6o**)**



¹³C NMR spectrum of **6o**

References

1. G. Kresse, J. Furthmüller, *Comput. Mater. Sci.*, 1996, **6** (1), 15–50.
2. P. E. Blöchl, *Phys. Rev. B*, 1994, **50** (24), 17953–17979.
3. G. Kresse, D. Joubert, *Phys. Rev. B*, 1999, **59** (3), 1758–1775.
4. J. P. Perdew, K. Burke, M. Ernzerhof, *Phys. Rev. Lett.* 1996, **77** (18), 3865–3868.
5. S. Grimme, S. Ehrlich, L. Goerigk, *J. Comput. Chem.* 2011, **32** (7), 1456–1465.
6. H. Bux, C. Chmelik, J.M. van Baten, R. Krishna, and J. Caro, *Advanced Materials*, 2010, **22**, 4741-4743.
7. Strauss, A. Mundstock, M. Treger, K. Lange, S. Hwang, C. Chmelik, P. Rusch, N.C. Bigall, T. Pichler, H. Shiozawa, and J. Caro, *ACS applied materials & interfaces*, 2019, **11**, 14175-14181.